# An Analysis of the Importance of Extension in Accounting for the Post-Carboniferous Subsidence of the North Sea Basin

By

John G. Sclater,
Steven J. Hellinger, and Mark Shorey

April 18, 1986

The University of Texas at Austin
Institute for Geophysics
4920 North IH 35
Austin, TX 78751

University of Texas Institute for Geophysics Technical Report #44

SUMMARY

Post Carboniferous sedimentary deposition in the Central North Sea basins can be separated into three major periods: Permian, Triassic and mid-Jurassic through present. Most efforts to explain the basin within an extensional framework have concentrated on the post mid-Jurassic subsidence. These efforts have ignored the large amount of prior extension required to account for the observed crustal thinning and the substantial Permian and Triassic sediment fill. In addition the models predict a mid-Jurassic through early Cretaceous extension that significantly exceeds estimates of the horizontal displacement observed on high angle faults on multichannel seismic lines.

We show in areas of minimal pre-Permian subsidence that adding two earlier phase extensions, one in the late Carboniferous through early Permian and the other in the Triassic produces a nearly horizontal late Carboniferous crustal thickness. The time-dependent extensional model required to account for the three periods of sediment deposition gives an excellent match to the observed subsidence history of the basement.

We present an analysis of a recent seismic reflection line run across the Central Graben in the vicinity of published refraction and well data. We show that the extension required in the third phase of the three phase model is compatible with the observed displacement on the high angle mid-Jurassic through early Cretaceous faults. However, we find no evidence for major extension either in the Triassic or late Carboniferous through early Permian.

The absence of visible evidence on the seismic line of major pre-Jurassic faulting is a problem. We propose that subsidence in the late Carboniferous was associated with wrench faulting and thermal destabiliza-

tion in the Tornquist Zone. The Triassic sediment fill resulted from transtensional faulting in same zone. Because both stages of faulting involve only fifteen to twenty percent extension and are in an area severely disturbed by later faulting, they will be difficult to detect. The depth of the faulted horizons, the substantial salt cover and possible later salt motion all add to these difficulties.

The three phase extensional model based on the geological history of the area accounts for the crustal thinning, the total sediment fill and the burial history of the basement. It should not be rejected because of the absence of evidence for major pre-Jurassic extension without a better understanding of the late Carboniferous and Triassic tectonic history.

INTRODUCTION

## Geologic history

The North Sea basin has been a site of major exploration for hydrocarbons. It is bounded by land masses whose geological history is well known. Also, there are abundant wells, logs and interpreted seismic sections available from the basin for study. Ziegler (1978) (1982) has published generally accepted summaries of the geological information of the area. Additional geophysical information is available. This includes gravity measurements (Donato and Tally, 1981) and deep crustal data. This data was gathered using both wide-angle (Barton and Wood, 1984) and normal incidence (Barton et al., 1984) methods. Simple models based on extension of the crust have provided a useful framework for examining the tectonic history of continental basins and shelves (Salveson, 1978; MacKenzie, 1978; and Royden, et al., 1980). Given that many of the major phases of subsidence appear related to prior extension and the abundance of geological and geophysical information, the North Sea basin is a particularly good area in which to test the quantitative validity of these models.

The sediments overlying crystalline basement in the North Sea accumulated in a suite of successive basins developed in response to varying tectonic settings (Ziegler, 1981). In much of the area, the basement was consolidated during the Caledonian orogeny which was followed by a period of Devonian faulting (Figure 1a). An early Carboniferous basin formed in the foredeep associated with the Variscan front. In the late Carboniferous compressional phase this basin was uplifted and eroded. The lower Carboniferous is generally taken as basement in the North Sea.

During the latest Carboniferous and early Permian (Stephanian-

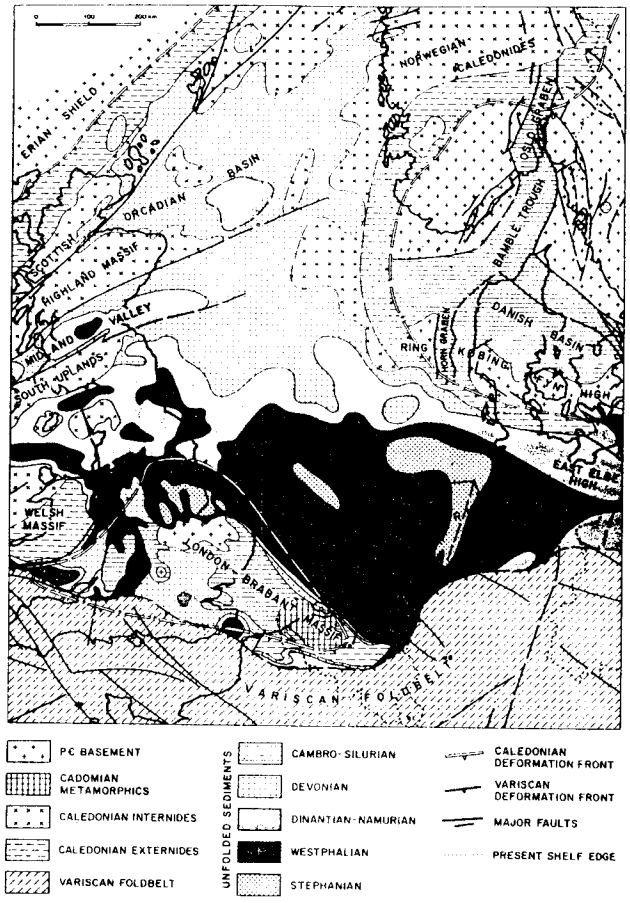


Figure 1a: Pre-Permian subcrop map of Northwestern Europe (Ziegler, in press).

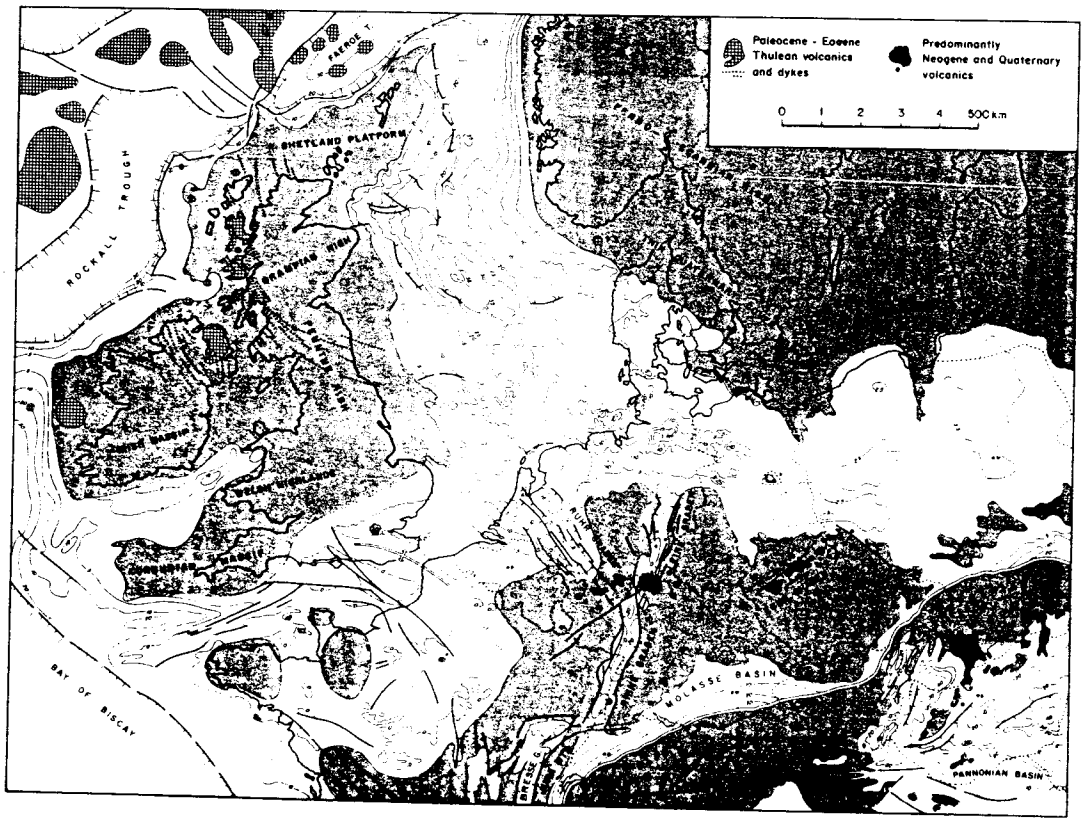


Figure 1b: Isopach map of Cenozoic series. Contours in hundreds of meters (Ziegler, 1981).

Autunian), there was a major phase of wrench faulting and igneous activity which profoundly changed the tectonic setting of the North Sea basin. Following this change, the east west trending north and south Permian basins were created. The general subsidence of these two basins gave rise to the deposition of the Rotliegend sandstone and the transgression of the Zechstein seas. During the Triassic, the North Sea was modified by the formation of a generally north-south graben system. However, in the region between the basin and the Russian-Fennoscandia platform (the Tornquist Zone), there is evidence for an east west trending system of half grabens (Ziegler, 1981, encl. 29; Pengrum, 1984; Figure 9).

The Viking and Central Grabens, which were created during the Triassic, developed during the Jurassic into the major structural elements in the North Sea. In the early Jurassic, there was apparent doming restricted to the Central Graben area before further extension started in the mid-Jurassic. Rifting and differential subsidence continued through the early Cretaceous to the mid-Cretaceous boundary. After this time, the subsidence in the basin became widespread with the thickest late Cretaceous and Tertiary sequences of sediments being deposited over the Viking and Central grabens. The Tertiary regional subsidence led to the development of the distinctive symmetrical saucer shape of the North Sea basin (Figure 1b).

We present as Figure 2a a schematic outline of the stratigraphy of the Central Graben (Ziegler, 1977) and in Figure 2b we show a correlation of the post-Triassic tectonic events in the North Sea with those in the North Atlantic and elsewhere in Europe (Ziegler, 1978).

There are five major periods of subsidence during the Phanerozoic in the North Sea basin: Devonian, Carboniferous, Permian, Triassic and upper Jurassic to present. The Triassic and post Jurassic subsidence is

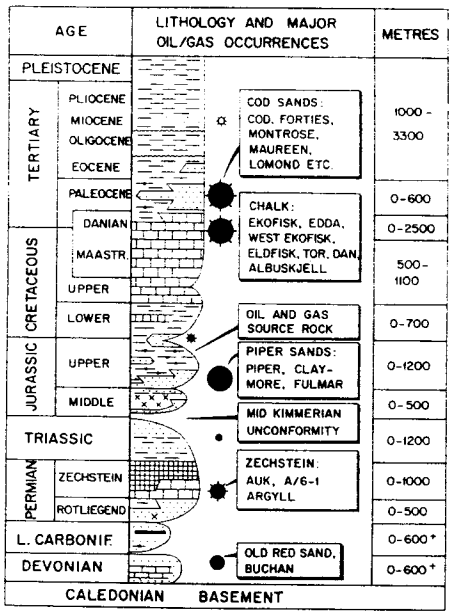


Figure 2a: A schematic outline of the stratigraphy of the Central Graben (Ziegler, in press).

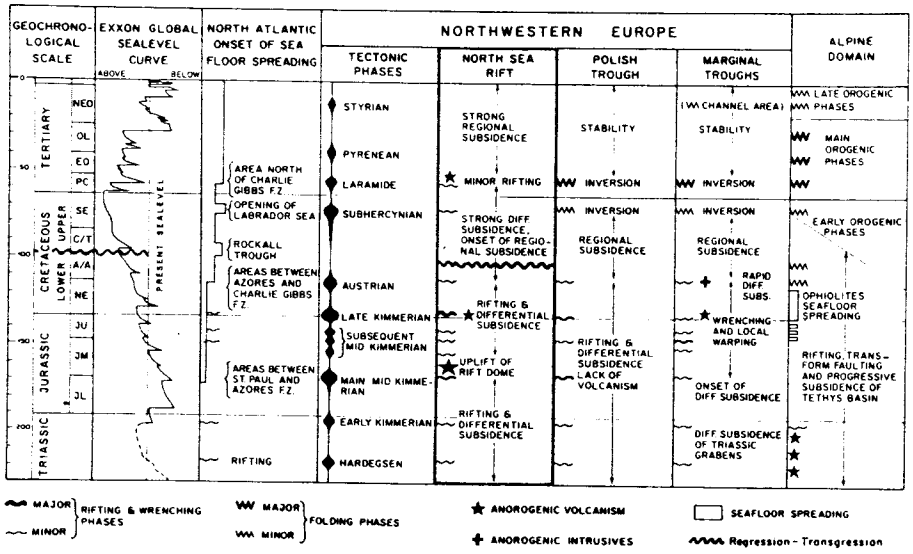


Figure 2b: Correlation of tectonic events in the Atlantic, the Northwestern European rift system and the Alpine orogenic belt (Ziegler, 1978).

associated with active faulting and extension. The Carboniferous subsidence is presumed related to the regional downwarping of the lithosphere at the toe of the Varisian front. There are differences of opinion as to how the Permian basins were created.

Glennie (1983) and Pegrum (1984) suggest that they were formed predominantly as a result of wrench faulting. In addition, Glennie (1983) believes they are related to all the post Permian phases of subsidence. On the other hand, Sorenson (in press) argues that both the north Permian basin and the Triassic Norwegian-Danish basin are predominantly thermal in origin and related to lithosphere wide cooling following the Stephanian-Autunian igneous event. Ziegler (1982) favors a combination of the two effects for the North Permian basin. He suggests a combination of wrench induced igneous activity followed by a thermal destablization of the lithosphere. Further, he argues that both the North and South Permian basins are not related to the Triassic phase of extension that led to the a creation of the Viking and Central Grabens.

The geological history presented by Ziegler (1982) separates the post lower Carboniferous tectonic activity into three separate phases involving extension and thermal destabilization to explain the Permian subsidence and extension for both the Triassic and post mid-Jurassic subsidence. As it is simple to relate these three phases directly to the observed subsidence pattern, we follow this history throughout the rest of this paper.

Definition of the problem

Various authors (Sclater and Christie, 1980; Wood, 1981; Wood and Barton, 1983) have applied the simple stretching concept as developed by McKenzie (1978) to the subsidence of the North Sea basin. Their efforts have concentrated exclusively on the post mid-Jurassic for two reasons. First, the visible high-angle fault breaks on industry multichannel seismic


Figure 3a: North Sea Permian and Mesozoic units.

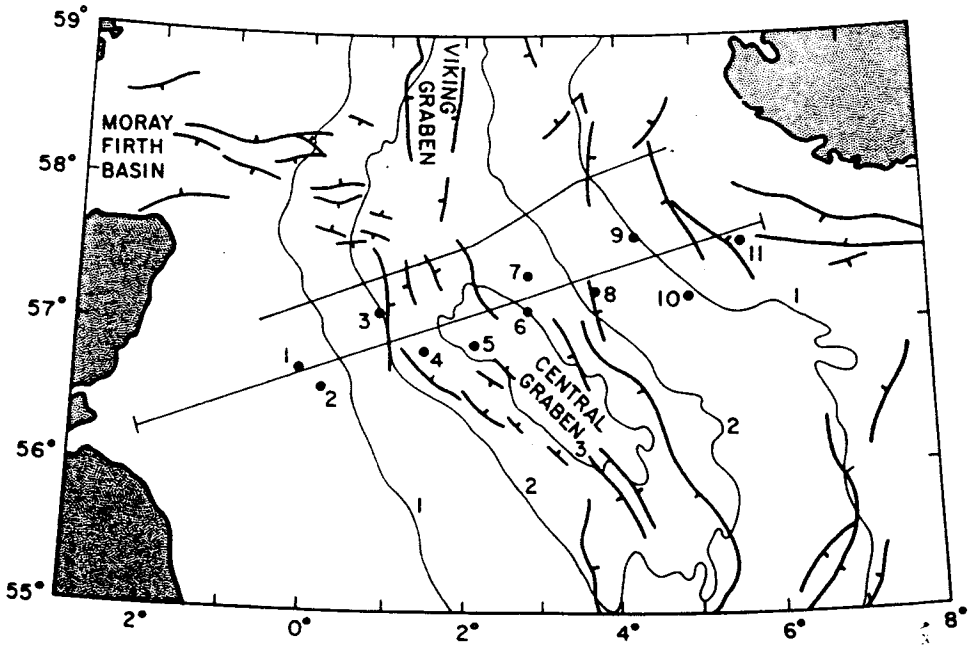


Figure 3b: Location map. Heavy lines: major faults, fine lines: Tertiary sediment isopachs in km, straight line: seismic refraction line from Wood and Barton (1983), numbered circles: well positions, Continuous line: NOPEC seismic line

lines provide clear evidence for mid-Jurassic through early Cretaceous extension. Second, the data base is more extensive and complete than that for any of the prior phases of subsidence.

Barton and Wood (1984) published a long-range seismic profile shot perpendicular to the Central Graben. In addition, they analyzed the data recovered from eleven exploration wells located close to the seismic line (Figures 3a and 3b). They observed a substantially thinner crust across the whole profile than that observed under the continents on either side. In particular, the crust was thinnest under the deep sedimentary fill of the Central Graben (Figure 4a). Along their cross section, they computed a 110 km increase in length assuming that the presently observed crustal thinning was due to extension. Further, they estimated that to explain the post mid-Jurassic subsidence they needed 50-80 km of this extension to occur during the mid-Jurassic through early Cretaceous phase of extension (Figure 4b).

More recently, Barton and Matthews (1984) have constructed the past thicknesses of the crust along the seismic profile. They assumed isostatic compensation and that the observed sediment fill was created by crustal thinning and extension. They found that the pre-Permian crust was thicker than that observed today. They argued that extension between the early Permian and the end of the Triassic created the crustal thinning. They related this phase of basin formation to the reactivation of a zone of Caledonian thrusts as low angle normal faults.

The isostatic calculations of Barton and Wood (1984) and Barton and Matthews (1984) imply a large amount of crustal thinning. The total amount of thinning is much larger than that required to explain the post mid-Jurassic subsidence. These calculations create a problem for the

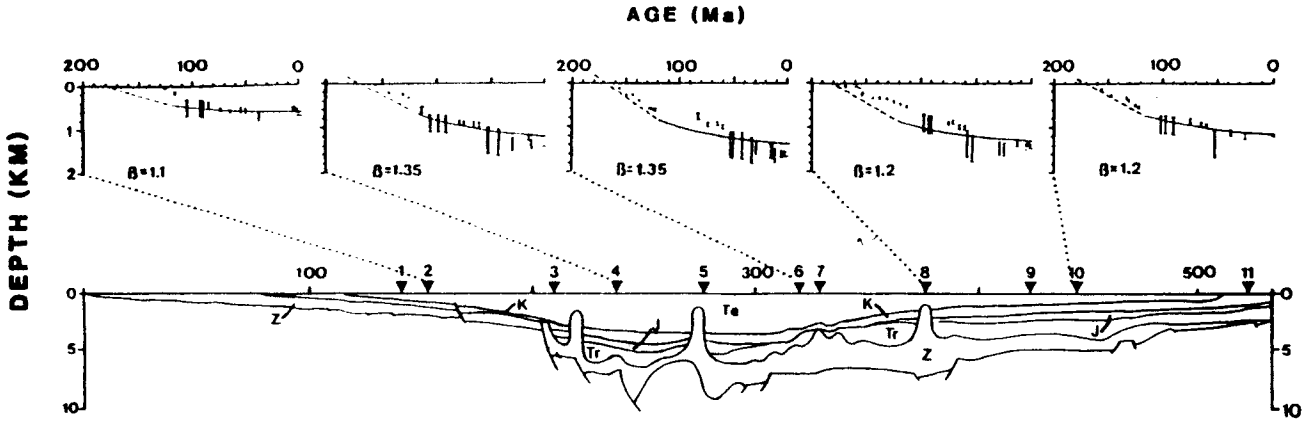


Figure 4a: Subsidence and structural data across the Central Graben.
Upper. Subsidence paths for five of the wells. Bars: range of basement level, dashed line: predicted fault-controlled subsidence, heavy line: predicted thermal subsidence, β value: estimate of crustal thinning (Wood and Barton, 1983).
Lower. Geological section along the seismic profile after Ziegler (pers. comm.) and Day et al. (1981). Te: Tertiary, K: Upper Cretaceous, J: Lower Cretaceous and Jurassic, Tr: Triassic, Z: Zechstein. Arrows indicate well position projected onto the line of section. Vertically exaggerated 5 times (Woods and Barton, 1983).

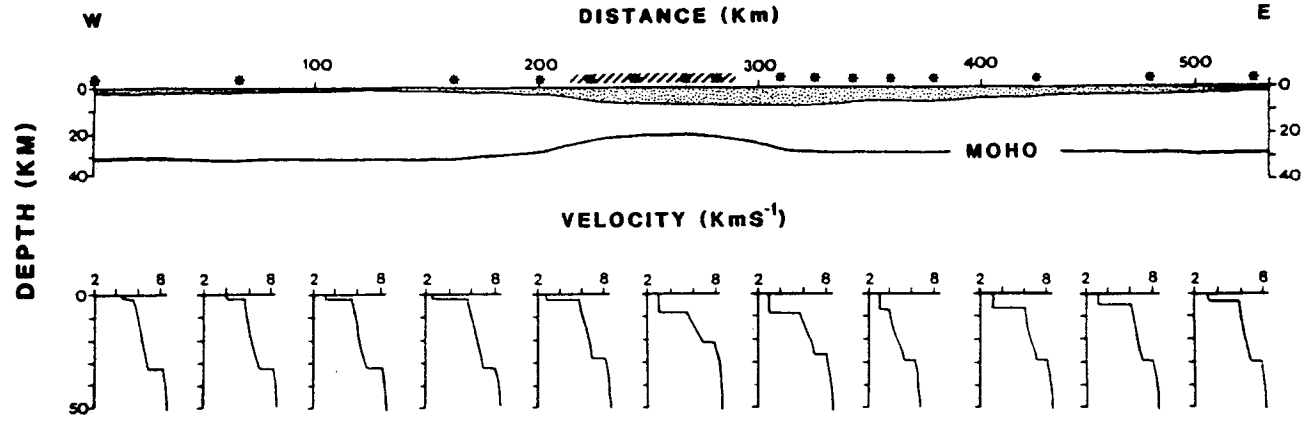


Figure 4b: Upper. Seismic crustal model, stipled area: Zechstein to recent sediments, heavy line: position of the Moho constrained to within 1 km, stars: shot points, slashed lines: PUSS array. No vertical exaggeration.
Lower. Velocity depth profiles at 50 km intervals along the seismic section, showing variation in crustal character with distance.

subsidence analysis of Wood and Barton (1983) since these authors reproduced the observed subsidence under the assumption that the thermal effects of any earlier event have completely decayed by the mid-Jurassic. This assumption permitted them to estimate the early Jurassic crustal thickness from the post mid-Jurassic subsidence without considering prior extension.

The seismic line (Wood and Barton, 1983) is located over the north Permian basin identified by Ziegler (1982) (Figure 5a). In addition, it lies close to the major axis of Triassic sedimentation in the region (Figure 5b). Between the latest Carboniferous and the latest Triassic there have been two major phases of extension and thermal destabilization. The second of the phases, in the Triassic, is sufficiently large that it will have created a thermal effect that cannot be ignored in computing the post mid-Jurassic subsidence. In the light of these new results the assumption of Wood and Barton (1983) that the thermal effect of any prior event will have almost completely decayed by the Jurassic is not justified by the observations.

Ziegler (1983) has raised a second problem which is not just restricted to the analysis of Wood and Barton (1983) but is general to all models seeking to explain North Sea subsidence by extension. Though unable to provide actual documentation because of difficulties with confidentiality, he has pointed out that the extension measured on high angle normal faults, visible on industry seismic lines across the Central Graben, is relatively small. The base of the Zechstein salt is a regionally correlative stratigraphic marker. Analysis of the offsets along this reflector has lead him to believe that extension by faulting at the level of this marker is probably 20-25 kms. He suggests it might be somewhat larger, but not by the factors of four or five necessary to

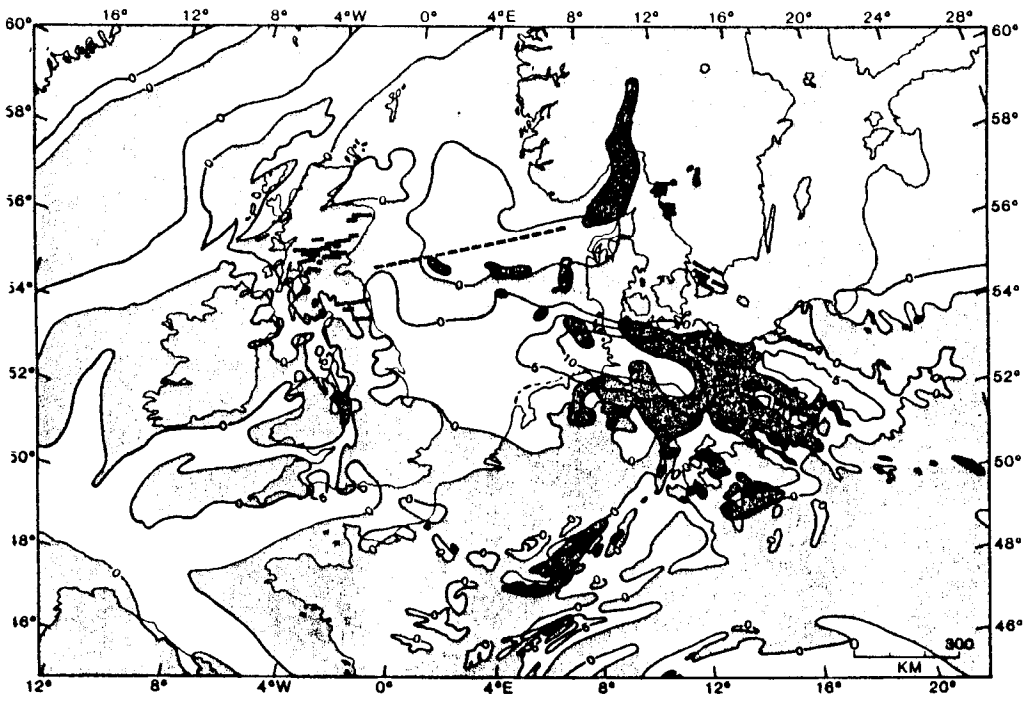


Figure 5a: Stephanian-Autunian Volcanics (shaded areas) and dyke swarms (horizontal lines), and a tentative isopach map of Rotliegend sediments, contour values in hundreds of metres.

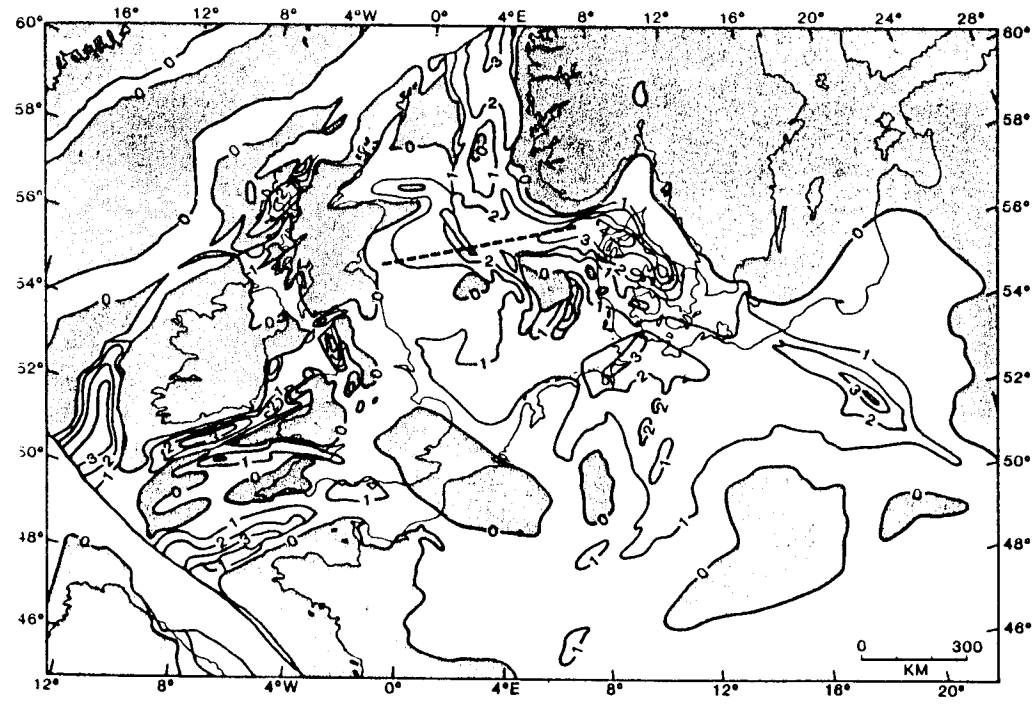


Figure 5b: Tentative isopach map of depositional thickness of Triassic sediments. Contour values in hundreds of metres.

account for the crustal thinning or subsidence. Further, most of the extension has occurred in th mid-Jurassic through early Cretaceous phase. He sites little direct evidence for major prior faulting.

Outline of the analysis

We have been given access by the Norwegian Petroleum Consulting Company (NOPEC) to a recent 'spec shoot' multichannel seismic line across the Central Graben in the vicinity of the refraction profile reported by Wood and Barton (1983) (Figure 3b). In our paper, we reexamine the subsidence of the North Sea basin in the light of the refraction and subsidence data presented by Wood and Barton (1983) and the crustal thinning calculations carried out by Barton and Wood (1984). We use the multichannel seismic line to address the problem raised by Ziegler (1983).

In presenting a simplified geological history of the Central North Sea basin, Ziegler (1981) recognizes three principle phases of faulting, extension and thermal destablization; Stephanian-Autunian, Triassic and mid-Jurassic through early Cretaceous. We attribute most of this thermal destabilization to extension and in matching observation with prediction consider the two earlier phases of extension as well as that between the mid-Jurassic and early Cretaceous.

Our analysis is separated into five major parts. First, we construct the thickness of continental crust in the pre late Carboniferous along the cross section of Wood and Barton (1983). Second, we show how to compute subsidence profiles from our time dependent extensional models. Third, we compute the total extension and separate it by phase. Fourth, we compare the observed and predicted subsidence. Fifth, we present a line drawing of the multichannel line across the Central Graben and illustrate where the seismic reflection data do or do not support our interpretation of the

refraction and subsidence data.

In this paper, we have chosen not to present any new well data or to justify in great detail the extensional model we have chosen as a framework. Our principal objective is to show that current subsidence, refraction and gravity data are well accounted for within an extensional framework, but that there are still problems matching the amount of extension required with the observed displacements of high angle faults on the multichannel seismic lines. Analyzing more or new subsidence data, creating a more elaborate extensional model, considering two dimensional effects and taking into account non-isostatic loading might slightly improve the fit of the observed and predicted curves. However, it would not in any way change the basic conclusions. In addition, as our objective is to limit the discussion to the pros and cons of an extensional framework, we do not discuss the data at all in the light of other models of subsidence. Ziegler (1983) has observed that extensional models predict more extension than is observed by conventional interpretation of seismic lines. This problem is not restricted to the North Sea. Royden et al. (1983), Hellinger et al. (1985) and Royden and Keen (1980) have raised a similar question in their analyses of, respectively, the Pannonian basin, the Bohai basin in China and the Labrador Shelf.

## DETERMINING THE PRE LATE CARBONIFEROUS CRUSTAL THICKNESS

In the Central North Sea basin the Caledonian basement is overlain by several hundred meters of Devonian shallow-water sandstones. The Devonian strata is covered by 5-10 km of Permian, Triassic and younger sediments. There are no Carboniferous strata. Permian strata start with the Early Permian Rotliegend sandstones. The shallow depth of deposition of the Devonian sandstones suggests that the basin was sediment-filled at that time. Carboniferous denudation of the area was probably modest, i.e., hundreds of meters rather than thousands (Ziegler, 1978; 1981). The pre-Permian subsidence was mainly restricted to the Devonian and is much less than that for the post-Carboniferous. We argue that in accounting for the subsidence pre-latest Carboniferous extension can be ignored and that only the Stephanian-Autunian, Triassic and mid-Jurassic through early Cretaceous phases need be considered.

The basin is in isostatic equilibrium and the flexural strength of the lithosphere is small (Barton and Wood, 1984). There is near total decay of the regional thermal anomalies generated by the three phases of extension. Thus, the observed subsidence of the early Permian basement reflects only crustal thinning and sediment loading. As a consequence the present crustal section may be used to construct the crustal structure at prior times (Barton and Wood, 1984; Barton and Matthews, 1984). Assuming point loading, with basement close to sea level, that extension took place in the plane of the section and that crust was conserved we extrapolated columns of the present crustal section backwards in time by removing successive thicknesses of the sedimentary units. Removing a layer of low density sediments requires isostatic compensation by crustal thickening. This is achieved by reducing the area of the basin. This reduction can be

perpendicular as well as parallel to the plane of the section.

We started with a geological cross section of the central North Sea basin (Figure 4a) and the observed thickness of pre-Jurassic crust from Table 1 of Wood and Barton (1983). The eleven sites along the cross-section are the locations of nearby wells (Wood and Barton, 1983). At each site we removed from the observed thickness of pre-Jurassic crust, first the thickness of the Rotliegend sandstones given by Ziegler (1982) and, then, the thickness of Zechstein (late Permian) salt and Triassic sandstone as measured from the cross-section. This gave us the presently observed thickness of the pre-late Carboniferous crust (Table 1). We reconstructed the crustal thickness prior to extension using the measured sediment thicknesses and appropriate sediment densities to compute the amount of crust removed (Table 1).

The pre-Permian crustal thickness lies within $\pm$ 3 km of 35 km. The 3 km variation is probably smaller than the actual uncertainties in our analysis caused by errors in the Moho depth (Barton and Wood, 1984), lack of knowledge of sediment properties, effects of salt motion and possible erosion of sediments. This crustal thickness is similar to the value of 35 km reported for the stable Permo-Scandian shield adjacent to the northeast end of the cross-section (Calcagnite, 1982).

The crustal thickness that we observe for the pre late Carboniferous is both thicker and involves much less scatter than that reported by Barton and Wood (1984). The reason for the difference is not known with certainty because they do not list the sediment thicknesses used in their calculations. We suspect that our thicker and more uniform crust is a result of our starting with a thicker total sediment fill. Our calculated pre late Carboniferous crustal thickness is closer to that reported on unextended crust to the east of the profile (Calcagnite, 1982). Both our

calculations and those of Barton and Wood (1984) imply substantial crustal extension. This extension occurred during the three phases of extension.

Table I Reconstruction of crustal thickness in the late Carboniferous

| Sites | 1 | 2 | 3 | 4 | 5 | 6 | 7 | 8 | 9 | 10 | 11 |
|---|---|---|---|---|---|---|---|---|---|---|---|
| Jurassic and younger sediment[1] | 1.0 | 1.2 | 3.7 | 4.8 | 4.8 | 3.7 | 3.0 | 2.6 | 2.2 | 2.2 | 1.5 |
| Triassic sandstone[1] | 0.0 | 0.0 | 0.7 | 0.9 | 0.5 | 1.0 | 1.0 | 1.6 | 1.3 | 1.5 | 0.9 |
| Zechstein (U. Permian) salt[1] | 0.9 | 0.7 | 1.5 | 3.3 | 3.6 | 2.0 | 2.3 | 2.5 | 1.8 | 1.6 | 0.5 |
| Rotliegend (L. Permian) sandstone[2] | 0.0 | 0.0 | 0.6 | 0.6 | 0.5 | 0.45 | 0.45 | 0.4 | 0.0 | 0.3 | 0.0 |
| Total sediment | 1.9 | 1.9 | 6.5 | 9.6 | 9.5 | 7.15 | 6.75 | 7.1 | 5.3 | 5.6 | 2.9 |
| Present thickness of late Carboniferous crust | 30.1 | 30.3 | 21.3 | 13.0 | 12.2 | 21.1 | 22.3 | 21.7 | 22.6 | 23.6 | 26.3 |
| A - assuming no compaction | | | | | | | | | | | |
| Average density[3] ($g\ cm^{-3}$) | 2.0 | 2.0 | 2.25 | 2.21 | 2.20 | 2.24 | 2.22 | 2.22 | 2.14 | 2.17 | 2.18 |
| Crustal thinning | 4.9 | 4.9 | 13.6 | 20.9 | 20.9 | 15.2 | 14.6 | 15.3 | 12.3 | 12.7 | 6.5 |
| Inferred thickness of late Carboniferous crust | 35.0 | 35.2 | 34.9 | 33.9 | 33.1 | 36.3 | 36.9 | 37.0 | 34.9 | 36.3 | 32.8 |
| B - assuming compaction | | | | | | | | | | | |
| Average density[3] ($g\ cm^{-3}$) | 1.94 | 1.95 | 2.23 | 2.25 | 2.22 | 2.21 | 2.16 | 2.15 | 2.10 | 2.13 | 2.04 |
| Crustal thinning | 5.2 | 5.1 | 14.0 | 20.3 | 20.5 | 15.6 | 15.4 | 16.4 | 12.7 | 13.1 | 7.3 |
| Inferred thickness of late Carboniferous crust | 35.3 | 35.4 | 35.0 | 33.3 | 32.7 | 36.7 | 37.7 | 38.1 | 35.3 | 36.7 | 33.6 |

Note: All entries in kilometers except for average density.

[1]Obtained from lithologic cross-section (Figure 1). Average depth of base Zechstein at site 3 was taken to be 6 km and at sites 4 and 5 was 9 km according to base Zechstein regional seismic structure map of Day et al.[14] At site 8 we interpolated the sediment horizons through the salt diapir.

[2]From Ziegler (1982).

[3]Obtained from weighted average of densities of four given layers. Layer densities were as follows. (a) Jurassic and younger sediments, sites 1, 2: 2 $g\ cm^{-3}$; sites 3-8: 2.3 $g\ cm^{-3}$; sites 9-11: 2.1 $g\ cm^{-3}$ (cf. Sclater and Christie) (b) Triassic sandstone; 2.4 $g\ cm^{-3}$, from Selley (c) Zechstein salt, 2.0 $g\ cm^{-3}$. (d) Rotliegend sandstone, 2.4 $g\ cm^{-3}$ from Selley.

[4]Computed using simple isostatic loading relation, $h = S[(\rho_m-\rho_s)/(\rho_m-\rho_c)]$ where h is the thickness of crust removed, S is the sediment-loaded basement subsidence (i.e., thickness of sediment column), $\rho_s$ is average sediment density, $\rho_c$ (=2.8 $g\ cm^{-3}$) is density of the crust and $\rho_m$ (=3.33 $g\ cm^{-3}$) is density of the mantle at the base of the unextended crust.

[5]Obtained from weighted averages of the four given layers. Layer densities were computed using the porosity depth relations given by Sclater and Christie (1980). The Jurassic and younger sediments were assumed to be sandy shales. The salt was given a density of 2.00 $g/cm^3$. The Triassic and Rotliegend sandstones were given the parameters of sands.

THE PREDICTED SUBSIDENCE

During and after extension, the basement subsides due to the thinning of the crust and the decay of the thermal anomaly which results from the thinning of the lithosphere. The total subsidence, $S_\infty$, can be separated into an initial subsidence, $S_{\Delta t}$, created during extension and the subsequent thermal subsidence, $S_t$.

McKenzie (1978) has evaluated $S_{\Delta t}$ and $S_t$ for different values of the extension parameter for the case of instantaneous extension. In addition, Le Pichon and Sibuet (1981) and Hellinger and Sclater (1983) have shown that in this case it is more useful to evaluate $S_\infty$ and $S_{\Delta t}$ in terms of $\gamma$. Hellinger and Sclater (1983, equations 3 and 6) present simple relations between subsidence $S_\infty$, $S_{\Delta t}$ and $\gamma$. These relations are easily modified to take account of varying crustal thickness, $t_c$.

Jarvis and McKenzie (1980) considered the case where stretching occurs over a finite time, $\Delta t$, at an exponentially increasing rate

$$\beta = e^{G\Delta t} \tag{1}$$

where G equals the magnitude of the vertical velocity gradient at the base of the lithosphere. They showed that for this case, there is a simple relation between $S_{\Delta t}$, the subsidence generated during extension, $\beta$, the extension factor, and $\Delta t$, the time over which extension occurs. This relation can easily be evaluated by combining the analysis of Jarvis and McKenzie (1980) with that of Hellinger and Sclater (1983) assuming, in the latter case, single layer extension. We do this in the following sections using the notation of Hellinger and Sclater (1983).

Jarvis and McKenzie (1980) evaluate the subsidence after extension terminates, $St(t,G')$ in terms of time t, a non-dimensional parameter $G'$, and $\Delta t$. $G'$ is related to $\beta$ and $\Delta t$ by the following equation

$$G' = a^2 \ln\beta / k\Delta t \qquad (2)$$

where a and k are, respectively, the thickness and thermal diffusivity of the lithosphere. The dimensionless parameter G' provides a relative measure of the velocities associated with stretching and thermal diffusion: $G'=\infty$ represents instantaneous extension. The post extensional subsidence for instaneous extension where $t=\infty$ is given the value $St_\infty (=St(t=\infty,G'=\infty))$ ($S_\infty$ in the notation of Jarvis and McKenzie, 1980). Jarvis and McKenzie (1980; Figures 6a and 6b) present curves of the ratio of $St_{G'} (=S(t=\infty,G'))$ ($S_G$ in the notation of Jarvis and McKenzie, 1980) the post extensional thermal subsidence for a given G', to $St_\infty$ for given values of G' or $\Delta t$. For a given $\beta$ and $\Delta t$ the ratio $St_{G'}/St_\infty$ has the scalar value f.

Subsidence during extension $S_{\Delta t}(t)$

$S_{\Delta t}$, the water loaded basement subsidence at the termination of extension, is related in a simple fashion to $S_\infty$, $S_i$ and f where $S_\infty$ is the total subsidence after infinite time ($S_{TOTAL}$ in Jarvis and McKenzie, 1980), $S_i$ is the basement subsidence immediately after instantaneous extension ($S_i$ in Jarvis and McKenzie, 1980), and f is as defined above. For example, the total subsidence is equal to the sum of initial and thermal parts, i.e.,

$$S_\infty = S_{\Delta t} + St_{G'} \qquad (3)$$

thus

$$S_{\Delta t} = S_\infty - St_{G'} \qquad (4)$$

Since f equals the ratio of $St_{G'}$ to $St_\infty$ then

$$St_{G'} = fSt_\infty \qquad (5)$$

and (4) becomes

$$S_{\Delta t} = S_\infty - fSt_\infty \qquad (6)$$

The post-extension subsidence for instantaneous extension, $St_\infty$, is given by

$$St_\infty = S_\infty - S_i \tag{7}$$

then (6) becomes

$$S_{\Delta t} = S_\infty - f(S_\infty - S_i) \tag{8}$$

Equation (8) relates the subsidence generated during extension to the initial and total subsidence for instantaneous extension through the scalar f. The scalar f for a given $\beta$ and $\Delta t$ are obtained directly from Figure 6b of Jarvis and McKenzie (1980). For arbitrary $\beta$, $S_i$ and $S_\infty$ can be computed from equations (3) and (6) of Hellinger and Sclater (1983). $S_{\Delta t}$ is always greater than $S_i$ because heat loss during the extensional phase creates additional subsidence.

It is more useful to present the relation between subsidence and extension in terms of the parameter $\gamma$ (Royden et al., 1980) where

$$\gamma = ( 1 - 1/\beta) \tag{9}$$

as there is a nearly linear relation between $S_{\Delta t}$ and $\gamma$ for $\gamma < \cdot 75$ ($\beta < 4.0$). We present as Figure 6 the relation between $S_{\Delta t}$ and $\gamma$, with $t_c$ equal to 35 km, for various values of $\Delta t$ between 25 and 200 m.y.

If the total amount of extension and the time interval over which extension occurred are known then $S_{\Delta t}(t)$, the initial subsidence during extension, can be determined. First G is evaluated from $\beta$ and $\Delta t$ using equation (1). Values of $\gamma$ for various values of time, t, less than the total time of extension, $\Delta t$, are computed. Then $S_{\Delta t}$ is determined by placing $\Delta t = t$ using equation 8. A faster and more convenient procedure is to read off $S_{\Delta t}$ directly from figure 6 for the appropriate value of $\gamma$ after setting $\Delta t = t$. This value of $S_{\Delta t}$ gives $S_{\Delta t}(t)$.

The inverse of this procedure can be used to determine $\gamma$. If the time interval over which extension took place and the basement subsidence during

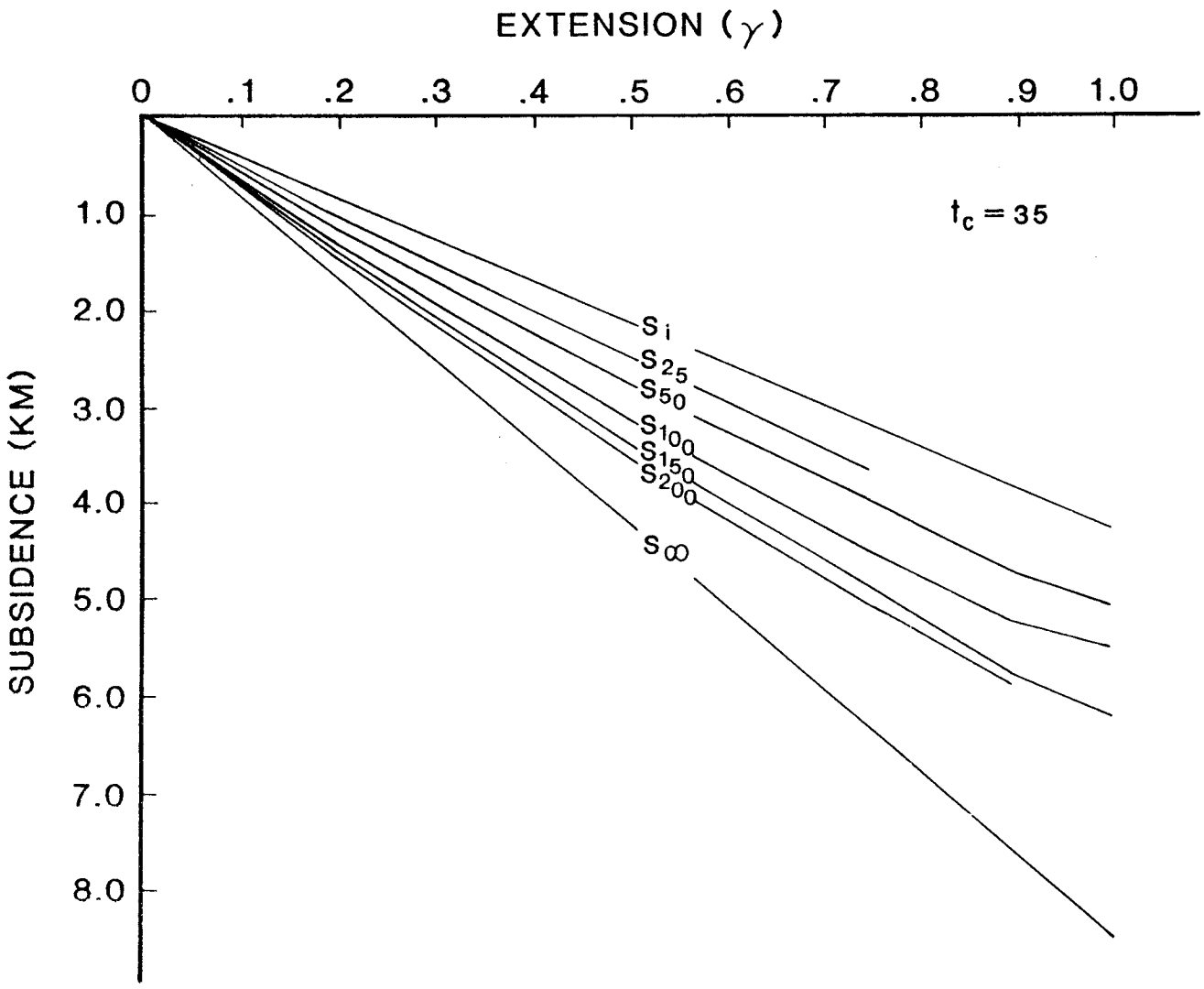


Figure 6. Relation between (water loaded) basement subsidence immediately after extension terminates, $S_{\Delta t}$, and the extension factor $\gamma$ for an initial crustal thickness of 35 kms and different values of $\Delta t$. $S_i$ is the basement subsidence achieved assuming instantaneous extension. $S_\infty$ is the total basement subsidence an infinite time after extension has ceased.

this time interval are known then figure 6 can be used to compute $\gamma$. Then $\beta$ is determined using equation 9.

Subsidence after extension terminates, $St(t,G')$.

The theoretical expressions given in Jarvis and McKenzie (1980) to determine the thermal subsidence after extension has terminated $St(t,G')$ are complicated and difficult to use. In the rest of this section we justify a simple method for evaluating $St(t\ G')$.

First, it is necessary to examine McKenzie (1978). In this paper McKenzie (1978) calculates the post extensional subsidence when stretching is instantaneous, i.e., $St(t,G'=\infty)$. He shows that for $\beta < 4.0$ the first term in the series expansion of e(t), the elevation at time t, dominates and that e(t) can be rewritten in the form

$$e(t) \cong E_o r \exp(-t/\tau) \tag{10}$$

where E is a constant depending upon the temperature and density of the upper mantle and the thickness and expansion coefficient of the lithosphere. r is a function of $\beta$. The subsidence after extension is given by the relation

$$St(t,G'=\infty) = e(o) - e(t)$$

$$\cong E_o r(1 - e(t)) \tag{11}$$

McKenzie (1978, Figure 3) demonstrated that the first term dominates by showing that for $\beta < 4.0$ a plot of $\log_{10} e(t)$ against t gave a straight line.

We examined Jarvis and McKenzie (1980 Figure 5) a plot of the subsidence $St(t, G')$ of a water filled basin against time for $\beta = 4$ and various values of G'. We computed e(t), the elevation relative to that after infinite time, for three values of G' (Table 2). We found that the values plotted on parallel straight lines (Figure 7). Thus, it is clear that the elevation, e(t), can be represented by an equation of the form

Table 2

Values of the subsidence after a finite extension time, the elevation relative to the total subsidence and the log of this elevation, for three values of G'

| $\sqrt{t - \Delta t}$ | 0 | 4 | 6 | 8 | 10 | 12 | 14 | ∞ |
|---|---|---|---|---|---|---|---|---|
| age | 0 | 16 | 36 | 64 | 100 | 144 | 196 | ∞ |
| G'=5, St(t,G') | 0 | .28 | .54 | .78 | 1.02 | 1.13 | 1.21 | 1.26 |
| e(t) | 1.26 | .98 | .72 | .48 | .24 | .13 | .05 | - |
| $\log_N$ e(t) | .231 | -.020 | -.33 | -.73 | -1.43 | -2.04 | 3.00 | - |
| G'=20, St(t,G') | 0 | .50 | 1.02 | 1.44 | 1.82 | 2.06 | 2.17 | 2.27 |
| e(t) | 2.27 | 1.77 | 1.25 | .83 | .45 | .21 | .1 | - |
| $\log_N$ e(t) | .82 | .57 | .22 | -.19 | -.80 | -1.56 | -2.30 | - |
| G'= α, St(t,G') | 0 | .68 | 1.31 | 1.86 | 2.34 | 2.64 | 2.80 | 2.94 |
| e(t) | 2.94 | 2.26 | 1.63 | 1.08 | 0.60 | .30 | 0.14 | - |
| $\log_N$ e(t) | 1.08 | .82 | .49 | .08 | -.51 | -1.20 | -1.97 | - |

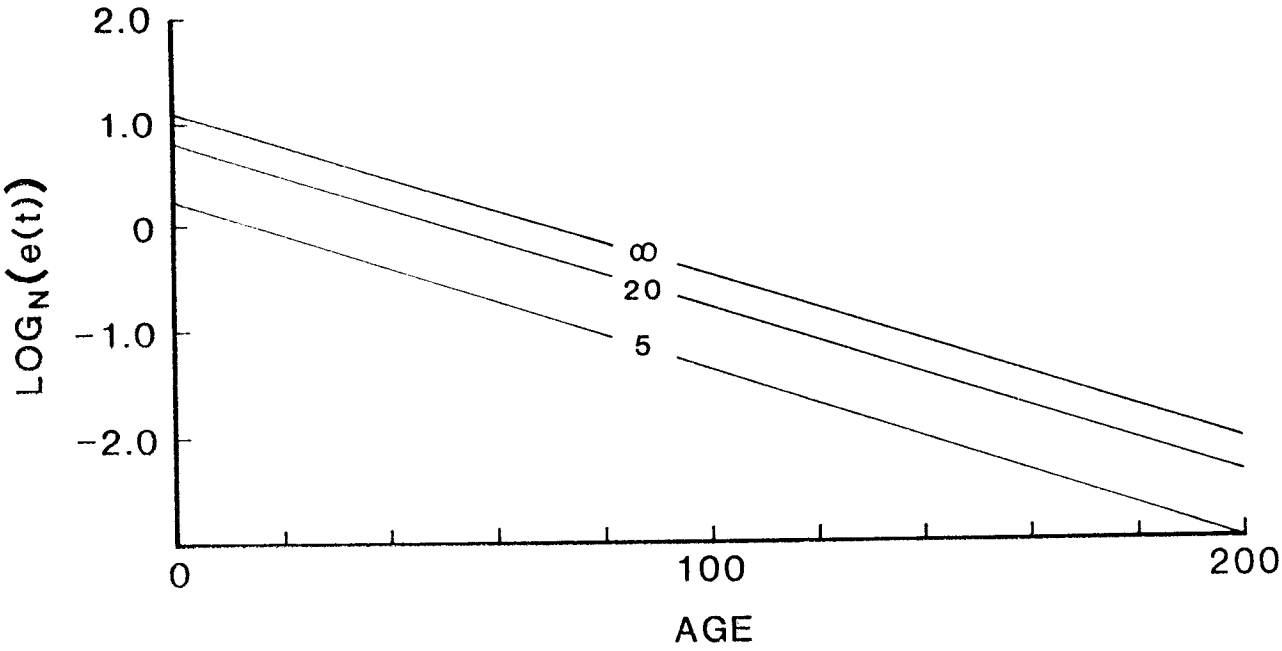


Figure 7. Plots of $\log_N$ (e(t)) against time for different values of G'. G'= ∞ indicates instantaneous extension.

$$e(t) \approx A\, e^{-t/\tau} \tag{12}$$

where $\frac{1}{\tau}$ is the slope of the $\log_N e(t)$ versus time plot and A is a constant.

Thus, the subsidence can be written

$$St(t,G') \approx A(1 - e^{t/\tau}) \tag{13}$$

where A is the total thermal subsidence at $t=\infty$. Thus

$$A = St(t=\infty,G') = St_{G'} \tag{14}$$

In the case of instantaneous extension (14) becomes

$$St(t,G'=\infty) \approx St_{\infty}\ (1 - e^{t/\tau}) \tag{15}$$

and for finite extension, $\Delta t$, (14) becomes

$$St(t,G') \approx St_{G'}(1 - e^{t/\tau}) \tag{16}$$

Dividing (17) by (16) we obtain

$$St(t,G') \approx \frac{St_G}{St_{\infty}}\ St(t,G'=\infty)$$

$$\approx f_{\infty}\ St(t,G'=\infty) \tag{17}$$

Thus, the subsidence after extension terminates is given by thermal subsidence in the case of infinite extension multiplied by the scalar f. f is determined directly from Jarvis and McKenzie (1980, Figure 6b) for the appropriate value of $\beta$ and $\Delta t$. The termal subsidence for instantaneous extension is determined directly from (McKenzie 1978, Equation 8).

The total subsidence, S(t) is given by the relation

$$S(t) = S_{\Delta t}(t) + St(t,G')$$

$$= S_{\Delta t}(t) + f_{\infty}\ St(t,G'=\infty) \tag{18}$$

It is computed by adding the thermal subsidence after extension to that created during the period of extension (Note that the approximation for the thermal subsidence has only been justified for $\beta<4.0$).

We present as Figure 8 a plot of the total subsidence through time for crust extended by a factor of four ($\beta$=4.0) for various values of the interval of extension, $\Delta t$. Note that for $\Delta t$ less than 20 m.y. there is less than 300 m difference in the value of initial subsidence between the case for instantaneous stretching and that when $\Delta t$ = 20 m.y. However as $\Delta t$ increases beyond 20 m.y. this difference increases and when $\Delta t$ is equal to 200 m.y. it is close to 2 km. These curves confirm the conclusion of Jarvis and McKenzie (1980) that for $\Delta t < 20$ m.y. assuming instantaneous extention is a valid assumption. For intervals of extension greater than this it is necessary to consider the effects of cooling during the period of extension.

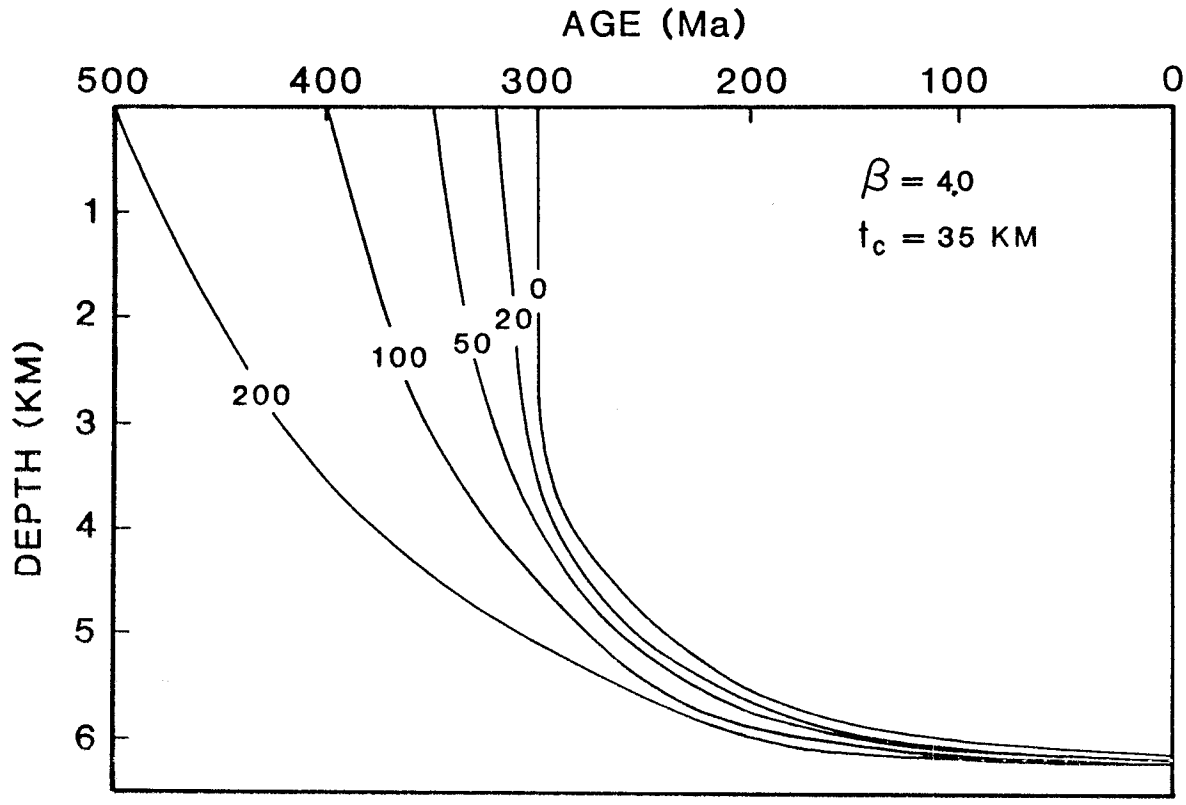


Figure 8. The total subsidence S(t) for five different intervals of extension for $\beta = 4.0$ and $t_c = 35$ kms. The numbers on the curves represent the time interval of extension in millions of years.

## CALCULATING THE PRE-JURASSIC AND POST TRIASSIC EXTENSION

We follow Ziegler (1982) and identify three major post mid Carboniferous phases of extension and thermal destabilization: Stephanian-Autunian, Triassic and mid-Jurassic through early Cretaceous. Further, we assume that only in the Stephanian-Autunian was thermal destabilization, associated with massive intrusion of basaltic material, important. Assuming pre late Carboniferous basement, the total amount of extension between the Stephanian and present is given by dividing the reconstructed pre-Permian crustal thickness by that for the present. Because of the lack of information about the pre-Permian subsidence and faulting, it is not possible to determine with any certainty the amount of extension in the Stephanian-Autunian. In addition, it is not possible to separate the thermal effects of the Stephanian-Autunian events from the effects of extension in the Triassic. Hence, it is not possible to separate the first phase of extension and thermal destabilization from the second phase of extension.

However, it is possible to separate the effects of the pre-Jurassic events from the later mid-Jurassic through early Cretaceous phase. To accomplish this we assumed that we could represent the Stephanian-Autunian faulting and thermal destabilization by simple extension. Further, we assumed that all the Triassic was created during active extension. If this is the case, then to a good approximation, the effect of both phases (Curve 1, Figure 9) can be combined into one phase of continuous extension (Curve 2, Figure 9). We assumed that all the pre-Jurassic subsidence is formed during extension. We can measure the basement subsidence from the late Carboniferous to the top of the Triassic. We know the interval of time over which extension took place. Thus we can calculate the amount of

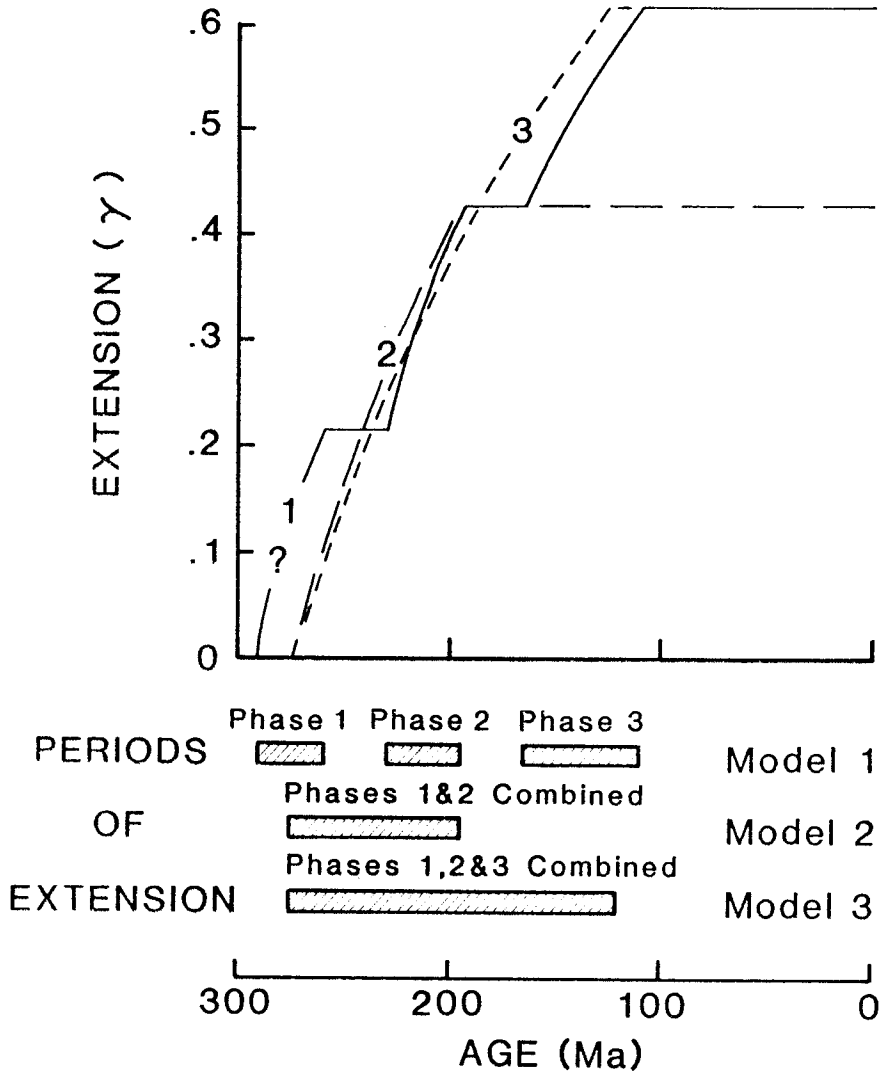


Figure 9. A plot of extension ($\gamma$) versus time for 3 different models. Model 1 represents the geological history of Ziegler (1982). Model 2 is the combination of phases 1 and 2 used to compute $\beta_{ST_r}$ (see text for explanation). Model 3 is the combination of phases 1, 2, 3 into one phase to compute the thermal subsidence between 110 Ma and present.

extension during this earlier phase.

To estimate the extension from the subsidence we assume a time dependent uniform extensional model with strictly vertical heat loss (Jarvis and McKenzie, 1980). We assume equilibrium lithospheric conditions before the first phase of extension because of minimal prior subsidence. The total extension factor, $\beta_T$, is related to those for the Stephanian through Autunian, Triassic and Jurassic through early Cretaceous phases, $\beta_{SA}$, $\beta_{Tr}$ and $\beta_{JC}$ respectively, as follows:

$$\beta_T = \beta_{SA}\beta_{Tr}\beta_{JC} \tag{20}$$

The late Carboniferous (pre-extension) crustal thickness divided by the present thickness of the late Carboniferous crust yields $\beta_T$.

As mentioned above, we have to consider the extension in the Stephanian through Autunian and Triassic as one phase, $\beta_{STr}$. To determine $\beta_{STr}$ we reduce (20) to

$$\beta_T = \beta_{STr}\beta_{JC} \tag{21}$$

By measuring the total basement subsidence between the Stephanian and the end of the Triassic and knowing, $\Delta t$, the time interval over which extension occurred $\beta_{STr}$ can be computed. $\beta_{JC}$ is determined from $\beta_{STr}$ and $\beta_T$ using (21).

We calculated the Stephanian through Triassic subsidence (Table 3a) by (a) determining the total (water loaded) subsidence from the total sediment thickness and average sediment density, (b) calculating the post Triassic subsidence from the thickness of Jurassic and younger sediments and (c) subtracting the post Triassic from the total subsidence (Table 1). These calculations assume that the basin was sediment filled at the end of the Triassic, that mid-Jurassic denudation was modest and that the pre Jurassic sediments did not compact beneath the overburden of younger sediments. The first two assumptions are reasonable (Ziegler, 1978; Ziegler, 1983). The

third is questionable. There is signigicant overpressure in the Central North Sea basin. Thus our assumption is not as unreasonable as it might first appear. To give a range to the maximum possible error introduced by the assumption we recomputed the basement subsidence assuming the porosity depth relations of Sclater and Christie (1980)(Table 3b). We computed the amount of crustal thinning for both cases.

In order to determine $\beta_{STr}$ it is necessary to select a time interval over which extension occurred and to measure the basement subsidence during this interval. We use the geological time scale of Van Eysinga (1975) to select the time interval as this scale assigns ages to the stage boundaries used by both Ziegler (1982) and Barton and Wood (1983). We place the onset of extension at the end of the Stephanian and the termination at the end of the Triassic (figure 9). This is a time interval of 80 m.y. starting at 275 and ending at 195 Ma.

We took the thickness of the various sedimentary layers presented in Table 1 and computed the water loaded basement subsidence under two different assumptions. First we assumed no compaction and constant densities. Then the calculations were repeated assuming compaction using the method and parameters given in Sclater and Christie (1980). The total Triassic and pre Jurassic basement subsidence at all eleven sites considered by Wood and Barton are presented in Tables 3a and 3b.

At each site, the initial crustal thickness was set equal to the reconstructed initial crustal thickness at that site (Table 1). This maintained consistancy between the model and the observed subsidence. However, it requires that the simple relation (8) between the initial subsidence for finite extension times be modified to account for varying crustal thickness. From Hellinger and Sclater (1983), it can be shown that

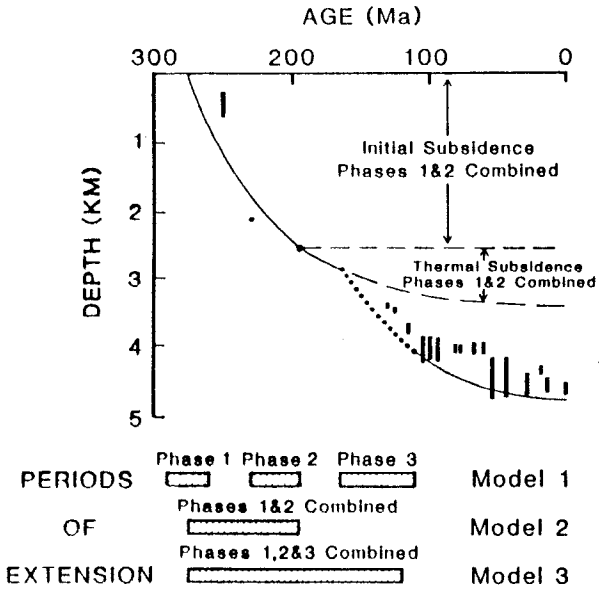


Figure 11a. The observed (water-loaded) basement subsidence at Site 4 compared with the subsidence predicted by three phases of extension - see Figure 10b for explanation. Filled circle represents the observed basement subsidence computed from the seismic profile, Figure 4a. 400 M has been added to the base of the Rotliegend sands to account for the water depth at this time. The thin rectangles represent the subsidence data of Wood and Barton (1983) superimposed on the subsidence history assuming the same basement depth for the present.

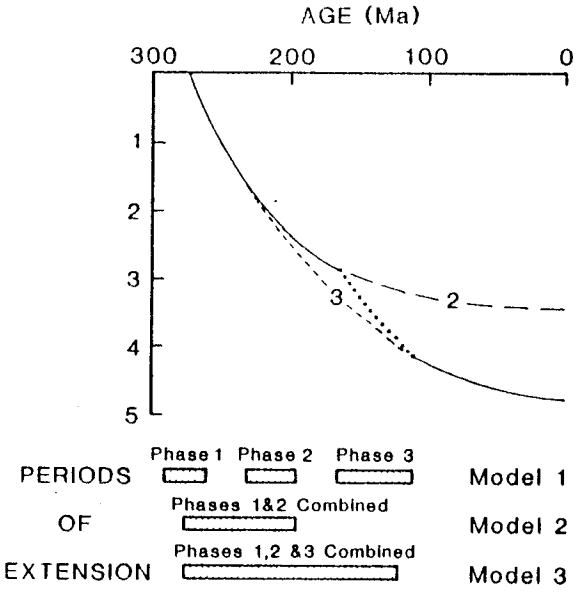


Figure 11b. The predicted (water-loaded) basement subsidence at Site 4. The periods of extension are shown below. Models 1, 2 and 3 represent respectively the geologic history of extension, the combination of phases 1 and 2 to compute $\beta_{STr}$ and the combination of phases 1, 2 and 3 to compute the thermal subsidence predicted by Model 2. The dashed line, 2, represents the thermal subsidence that would have occurred had there been no third phase of extension. The solid curve, 3, represents the thermal subsidence between 110 Ma and present calculated using Model 3. The light dashed line represents the earlier subsidence from the same model. The dotted curve is a straight line drawn between the basement subsidence at 165 Ma from 1 and 110 Ma from 3. It represents the subsidence during extension of the third phase. A crustal thickness of 34 km was assumed throughout.

sandstone may underestimate the basin subsidence. We added 400 M to the basement subsidence at the base Rotliegend to account for the water depth at this time (Glennie, 1984). The Zechstein sediments accumulated under gradually shallowing-upward conditions and by the end of the Permian sedimentation was probably in balance with subsidence. This balance was maintained during the Triassic (Ziegler, 1982). Basement subsidence was rapid during the late Permian and somewhat slower during the Triassic.

We determined the predicted subsidence by assuming that the subsidence through the Permian and Triassic occurred during a single phase of extension and that it could all be considered initial. Using Figure 10a and assuming a crustal thickness of 34 km we arrived at a value of .43 for $\gamma_{STr}$. From (9) this gives a value of 1.75 for $\beta_{STr}$. As the time interval for extension is 80 m.y. G can be determined from (1). Knowing G it is possible to compute $\gamma$ at earlier times during extension and to determine $S_{\Delta t}(t)$ from Figure 10a. We computed the subsidence during extension combining phases 1 and 2 into a single phase (Model 2, Figure 11b). This predicted subsidence gives a good fit to the observations (Figure 11a) because most of the crustal thinning and hence the initial subsidence has been placed in the early past of the extensional phase.

After the cessation of extension in the Triassic there was gradual thermal subsidence due to decay of the thermal anomaly created by this extension (Figures 11a and b). If there had been no mid-Jurassic through early Cretaceous extension then the basement would have subsided to a (water-loaded) depth of approximately 3.3 km upon complete decay of the thermal anomaly. Near-complete decay of the thermal anomaly would have occurred about 200 m.y. after the cessation of extension and therefore the present basement subsidence would have been approximately 3.3 km. The difference between this total subsidence (3.3 km) and the initial

subsidence (2.51 km), approximately .8 km, would have been the thermal subsidence due to the first phase of extension (Figures 11a and b). Thus a significant proportion of the post mid-Jurassic subsidence is due to thermal subsidence from the first extensional phase. Estimates of mid-Jurassic through early Cretaceous extension that do not take this subsidence into account will be much to large.

The third phase of extension began in the mid-Jurassic (165 Ma) and ended in the early Cretaceous (110 Ma). By 165 Ma the basement had undergone 80 m.y. of extension followed by 30 m.y. of thermal subsidence and had subsided to a (water-loaded) depth of approximately 2.9 km. At that time basement depth diverged from the thermal subsidence curve of the first two phases combined. By 110 Ma it had attained a depth approximately 4 km (Figure 11a dotted line between 165 and 110Ma). From 110 Ma to the present we had renewed thermal subsidence and the basement depth increased from 4 km to 4.7 km.

We have predicted the subsidence from 275 Ma to 165 Ma by combining the first two phases of extension into one phase lasting 80 m.y. It is beyond the scope of this paper to add the effect of the third phase of extension between 165 and 110 Ma directly to the subsidence predicted for the first two phases combined. To simplify the analysis we have computed the subsidence assuming that the effects of all three phases can be combined into one phase (Model 3, Figure 9 and Figures 11a and b). We assumed continuous extension of amount between 275 and 125 Ma. We recomputed the initial subsidence by recalculating G and evaluating S (t) for the appropriate values of using Figure 10b, a plot of initial subsidence versus for various values of t for a fixed value of $t_c$ equal to 150 m.y. Then, we assumed that the thermal subsidence given by this one

phase continuous stretching between 110 Ma and present is the thermal subsidence for the three phases combined. This assumption is reasonable as the proposed continuous extension is a reasonable approximation to the three phases considered individually (figure 9). As we cannot predict with any certainty what happens between 165 and 110 Ma., we have joined these two depths by a straight line when computing the predicted depths.

The total subsidence that we predict using this continuous extension model for phases 1, 2 and 3 gives a good match to the burial history of the basement. It also gives a good match to the total subsidence observed at Site 4. We made the same assumptions at the other four sites considered by Wood and Barton (1983). The overall match between the observed and predicted burial history is good (Figure 12). However at Sites 8 and 10 adding the Wood and Barton (1983) data appears to imply uplift in the early Jurassic. At the present stage of analysis it is not known whether this is real or an artifact of our analysis. For example, had we used different densities for the Triassic and Rotliegend sandstones most of this effect could have been removed.

The match between the observations and predictions is good. Clearly the three phase extensional and thermal distabilization history as proposed by Ziegler (1982) and modified by us can give a good fit to the overall burial history as well as accounting for the crustal thinning.

At our present understanding of the pre Triassic history of the Central North Sea it is not possible either to separate the Stephanian-Autunian phase of extension and thermal destabilization from that in the Triassic. In addition it is not possible to tell from the subsidence alone whether extension or thermal destabilization along the lines of Royden et al., (1981, Model 3) was the dominant mechanism for subsidence during the Stephanian and Autunian.

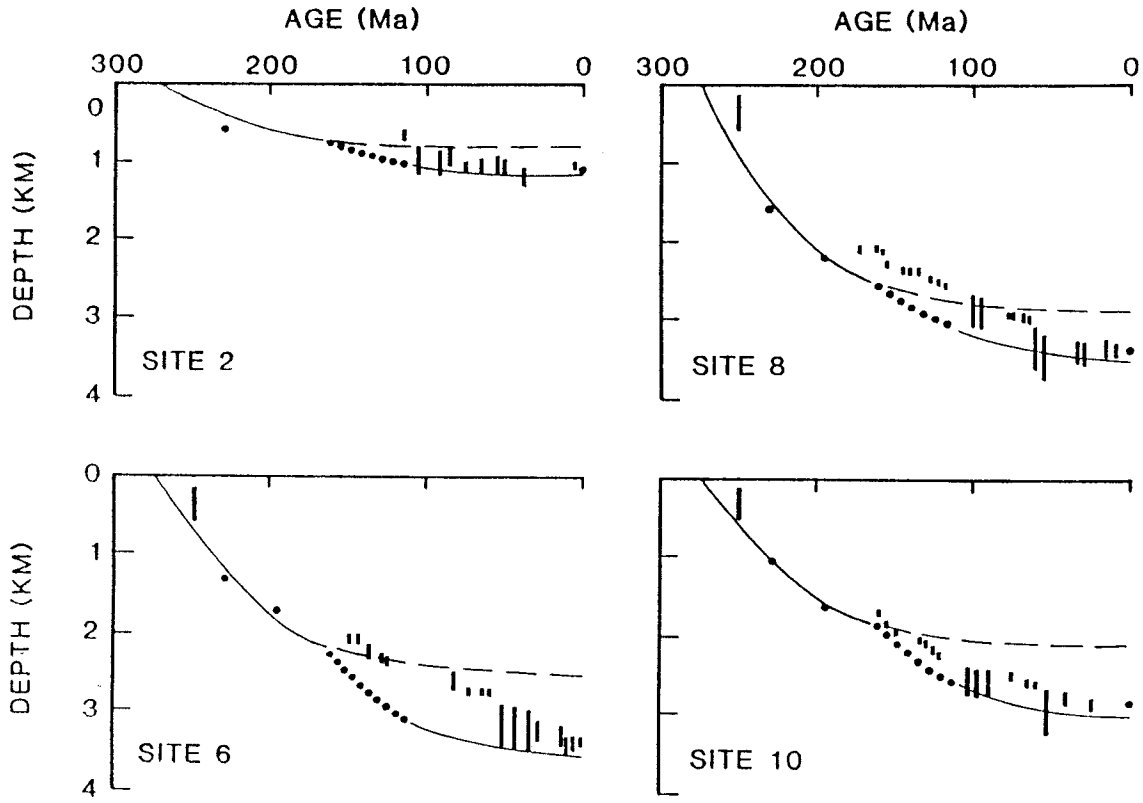


Figure 12. Comparison of predicted (water loaded) basement subsidence with observed subsidence for sites 2, 6, 8 and 10.

## EXTENSION OBSERVED ON SEISMIC REFLECTION RECORDS

The degree of crustal extension beneath the central North Sea basin has been obtained from calculations of the amount of crustal thinning and the variation of the sediment thickness through time. These calculations yield crustal extension parameters which can account for the observed subsidence history.

Another method of obtaining these parameters is to examine the throw on faults active during extension. Recently the Norwegian Petroleum Exploration Consultants (NOPEC) gave us a seismic line across the Central Graben. They shot this line just north of the refraction profile and well data presented by Wood and Barton (1983) and Barton and Wood (1984). They acquired the data during a 'spec shoot' survey of the Central Graben using a super wide airgun array and a 3 km long streamer. The location of the line can be found on Figure 3b. The migrated time section is presented as Figure 13a and also as a fold out in the back of this report.

We interpreted the section using released well data, composite logs from the wells and an interpreted seismic section from the Montrose field (Fowler, 1975). We had additional help in interpreting this section from NOPEC, Phillips Petroleum Company, and A. W. Bally of Rice University. A line drawing of the section is presented as figure 13b and on the fold-out.

As this section is to be interpreted in more detail elsewhere (Shorey and Carstens, in preparation) we present here only a short summary of the major features of the profile. We start with the present and work backwards in time. The dominant feature of the Cenozoic and late Mesozoic is the pervasive subsidence and sedimentation which commenced at the beginning of the deposition of the mid-Cretaceous chalk and has continued until the present. The only major tectonic activity during this time span

Table 3a Pre-Jurassic and Mid-Jurassic - early Cretaceous extension, assuming no compaction

| Sites | | 1 | 2 | 3 | 4 | 5 | 6 | 7 | 8 | 9 | 10 | 11 | |
|---|---|---|---|---|---|---|---|---|---|---|---|---|---|
| Total subsidence[1] | | 1.10 | 1.09 | 3.05 | 4.67 | 4.67 | 3.40 | 3.25 | 3.42 | 2.75 | 2.84 | 1.45 | |
| Post Triassic subsidence | | 0.58 | 0.69 | 1.66 | 2.16 | 2.15 | 1.66 | 1.34 | 1.16 | 1.18 | 1.18 | 0.80 | |
| Pre-Jurassic subsidence | | 0.52 | 0.40 | 1.39 | 2.51 | 2.52 | 1.74 | 1.91 | 2.26 | 1.57 | 1.66 | 0.65 | |
| | | | | | | | | | | | | | $\beta^{-3}$ |
| Extension factor $\beta$[2] | Total | 1.16 | 1.16 | 1.64 | 2.61 | 2.71 | 1.72 | 1.65 | 1.71 | 1.54 | 1.54 | 1.25 | 1.70 |
| | SA-$T_r$ | 1.11 | 1.10 | 1.28 | 1.75 | 1.82 | 1.41 | 1.45 | 1.52 | 1.32 | 1.32 | 1.14 | 1.38 |
| | mJ-$\varepsilon$C | 1.05 | 1.05 | 1.28 | 1.49 | 1.49 | 1.22 | 1.14 | 1.13 | 1.17 | 1.17 | 1.10 | 1.21 |

[1]The isostatic loading relation for water loaded subsidence is equal to $S[(\rho_m-\rho_s)/(\rho_m-\rho_w)]$ where $\rho_w$ is water density and other items are defined in Note 4 of Table 1.

[2]Initial crustal thickness is given in Table 1. SA- $T_r$ and mJ - $\varepsilon$C are respectively the Stephanian-Triassic and Mid-Jurassic - early Cretaceous phases.

[3]The mean extension factor.

Table 3b Pre-Jurassic and Mid-Jurassic - early Cretaceous extension, allowing for compaction

| Sites | | 1 | 2 | 3 | 4 | 5 | 6 | 7 | 8 | 9 | 10 | 11 | |
|---|---|---|---|---|---|---|---|---|---|---|---|---|---|
| Total subsidence[1] | | 1.15 | 1.14 | 3.12 | 4.53 | 4.58 | 3.47 | 3.43 | 3.64 | 2.83 | 2.91 | 1.62 | |
| Post Triassic subsidence | | .63 | .74 | 1.32 | 1.65 | 1.72 | 1.27 | 1.09 | 0.87 | 0.84 | 0.78 | .67 | |
| Pre-Jurassic subsidence | | .52 | .40 | 1.80 | 2.88 | 2.86 | 2.20 | 2.34 | 2.77 | 1.99 | 2.13 | .95 | |
| | | | | | | | | | | | | | $\beta^{-3}$ |
| Extension factor $\beta$[2] | Total | 1.17 | 1.17 | 1.64 | 2.56 | 2.68 | 1.74 | 1.69 | 1.76 | 1.56 | 1.56 | 1.28 | 1.71 |
| | SA-$T_r$ | 1.11 | 1.10 | 1.41 | 2.00 | 2.08 | 1.53 | 1.56 | 1.68 | 1.47 | 1.45 | 1.19 | 1.51 |
| | mJ-eC | 1.05 | 1.06 | 1.16 | 1.26 | 1.29 | 1.14 | 1.08 | 1.05 | 1.06 | 1.08 | 1.07 | 1.12 |

[1,2] and [3] as above.

if $t_c$ is the crustal thickness

$$S_i \approx 0.2077\ t_c\gamma - 0.0334\ (125 - t_c)\gamma \qquad (22)$$

and

$$S_\infty = 0.241\ t_c\gamma \qquad (23)$$

The relationship between $S_{\Delta t}$ and $\gamma$ is still close to a straight line. We present as Figure 10a this relationship for $\Delta t$=80 and $t_c$ varying in steps of 1km from 32 to 38km in thickness.

We used Figure 10a, the original crustal thickness and the pre Jurassic subsidence to determine $\gamma_{STr}$. We computed $\beta_{STr}$ using (9) and then used (21) to determine $\beta_{JC}$. A specific example, Site 4, is discussed later in the text (Figure 11). At sites 1, 2, 6 and 7 we made a correction of 150M for the erosion of the Triassic sediments during mid-Jurassic uplift and exposure (Ziegler, 1983; Leeder, 1983).

The extension factors that we have derived from the subsidence (Table 3) show a significant range depending upon whether or not we assume compaction in the Triassic or Rotliegend sands. If no compaction is assumed then about 40 percent of the extension occurrs in the mid-Jurassic through early Cretaceous phase. If the sediments are assumed to compact only about 20 percent of the extension occurrs during this phase. This range in extension is relatively large and indicates that any calculation of exact value for this or the earlier phases of extension should be treated with caution. However, two conclusions general to both sets of calculations can be drawn. First, there is greater extension before the Jurassic than in the mid-Jurassic through early Cretaceous phase. Second, in this last phase, extension was restricted mainly to the Central Graben and was small on the flanks.

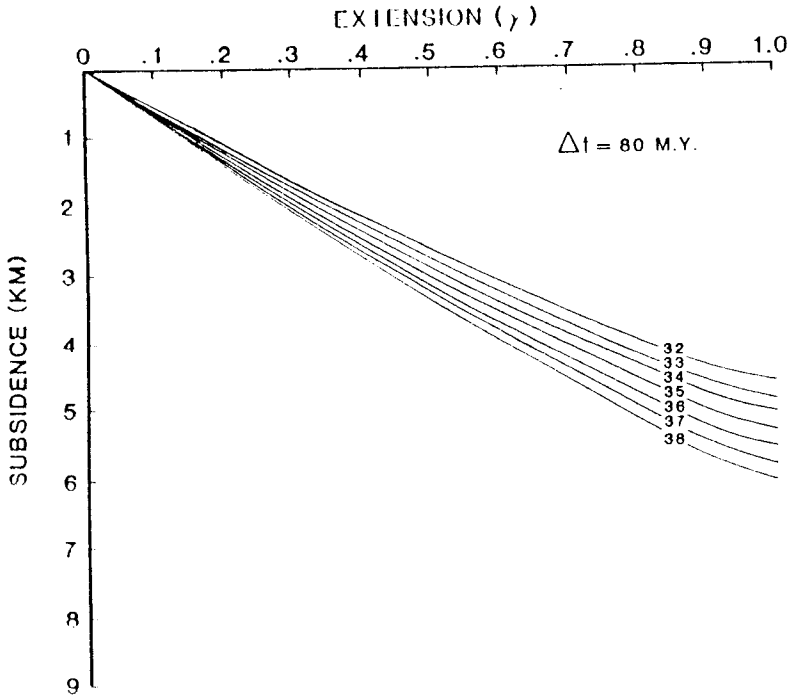


Figure 10a. The relation between (water loaded) basement subsidence during extention, $S_{\Delta t}$, and $\gamma$ for various values of crustal thickness, assuming a single time interval of 80 my for the period of extension.

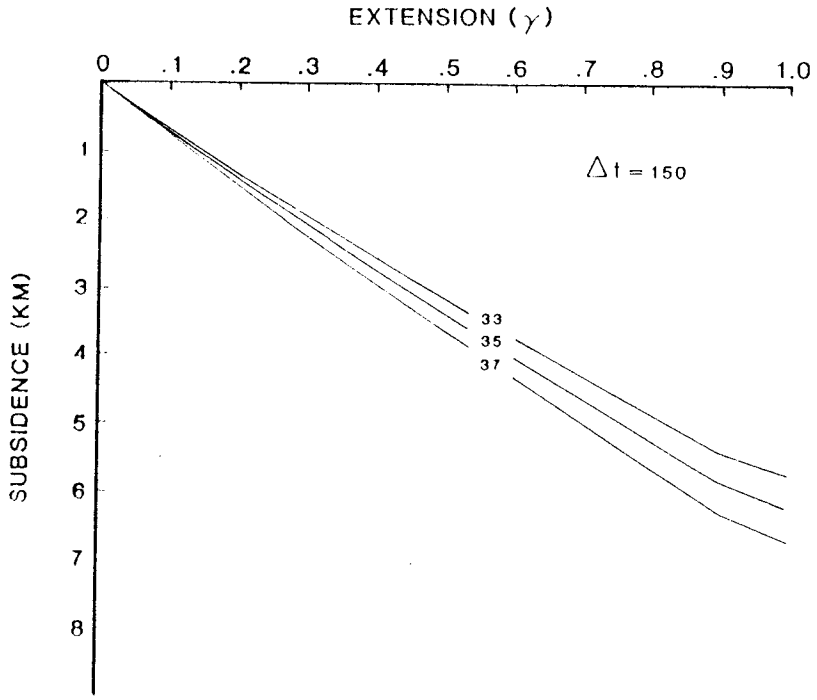


Figure 10b. The relation between (water loaded) basement subsidence during extension, $S_{\Delta t}$, and $\gamma$ for various values of crustal thickness assuming a time interval of 150 My for the period of extension.

## COMPARISON OF OBSERVED AND PREDICTED SUBSIDENCE

We determined the observed subsidence history at each of the five sites considered by Wood and Barton (1983) by measuring the depths of the Jurassic, Triassic and Zechstein from the seismic profile (Figure 4b). We took the thickness of the Rotliegend sands from Ziegler (1982). The individual layers were removed and the load of the resultant sediment column was subtracted assuming point loading. This gave the water loaded basement subsidence history.

Wood and Barton (1983) have provided a detailed subsidence history for the post mid-Jurassic at each of five wells located near their refraction profile (Figure 4a). Their analysis included error estimates on the depth of deposition. We added their analysis of the depths between the Jurassic and present (rectangles, Figures 11a and 12) to our analysis of the seismic horizons by assuming the same unloaded basement depth for the present. There are errors involved with this procedure as the wells and sites are not located exactly at the same place and different figures have been used for the densities of the deeper layers. However, the overall agreement is good and adding their data significant our confidence in the overall trend of the basement subsidence curves.

We illustrate the procedure followed to match the observed subsidence with the predicted by simple extension by considering Site 4 in some detail. The total subsidence between the early Premian and Triassic at this site was 2.51 km (Table 3; Figure 11a). This represents the initial subsidence during the first two phases of extension. The Zechstein was assumed not to have compacted on burial. There is a problem at the base of the Rotliegend because basement subsidence may have outpaced sedimentation during the early Permian (260-250 Ma). Thus, thickness of Rotliegend

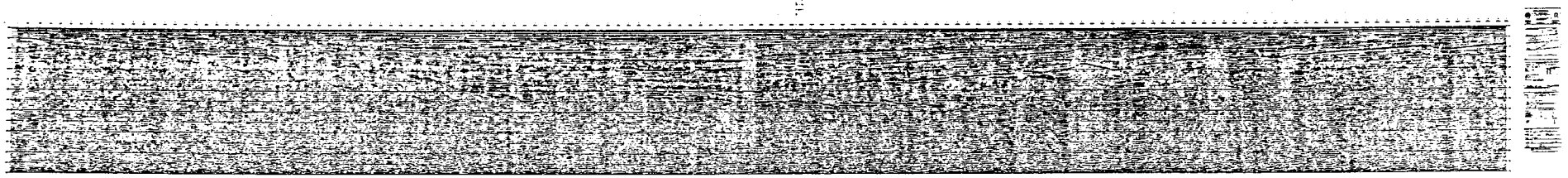

Figure 13a: NOPEC CNST 82-02 seismic line across the Central Graben in the North Sea. Data acquired using a super wide array with 60 hydrophone groups per cable and 40 hydrophones per group. The cable length was 3010 meters and the shot interval was 50 m. This is a migrated section. The location of the profile is shown on Figure 3b.

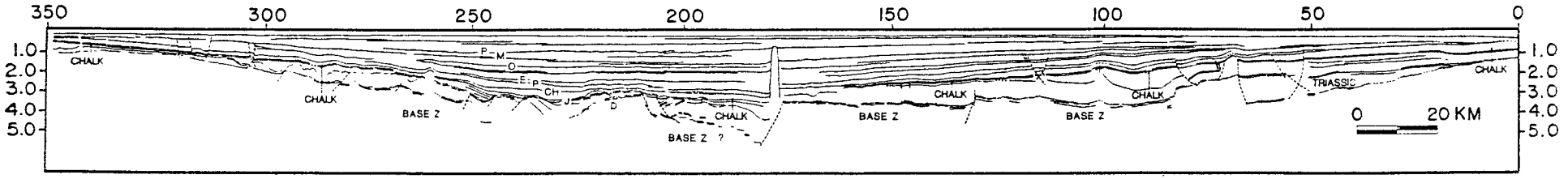


Figure 13b: A line drawing interpretation of NOPEC CNST-82 based on well information and seismic profiles. Note the mid-Jurassic through early Cretaceous faulting in the center of the profile indicating the Central Graben. Also note the continuity of the base Zechstein horizon either side of the Central Graben.

is salt diapirism. The major period of faulting observable on the seismic profile appears to have occurred from the mid-Jurassic through the early Cretaceous. Some of the faults are major especially the one on the western flank of the graben. The Jurassic sequences are thin in contrast to the thicker Triassic and Permian sequences. The Jurassic shows striking evidence for erosion both on the flanks and on the horst in the center of the graben. The sedimentary sections are underlain by a clearly identifiable pervasive base Zechstein (salt) reflector which extends both to the east and west of the graben. There is evidence that this reflector is observed within the graben on either side of the central horst.

There is considerable evidence from the seismic line for mid-Jurassic through early Cretaceous extension but very little obvious evidence for any major earlier phases. To compare the observed extension on the high-angle faults with that from the crustal and subsidence studies we redrafted the interpretation of the seismic line emphasizing respectively the mid-Jurassic through early Cretaceous and Permian and Triassic faulting (Figure 14). We divided this section into three regions: western flank (350-250 km),central Graben (250-150 km) and eastern flank (150-50 km). We measured the horizontal displacements within each region and computed the extension factor for each phase of the faulting (Table 4). We compared these results with the average values of $\beta_{JC}$ for wells lying within each region (Table 4). We obtained a range in the average extension factor for this latter calculation by considering the cases where the sediments do and do not compact. The fault-derived extension factors for the mid-Jurassic through early Cretaceous phase are in good agreement with those derived from the crustal thinning and subsidence data. Both sets of data indicate between 30 and 40 km of extension.

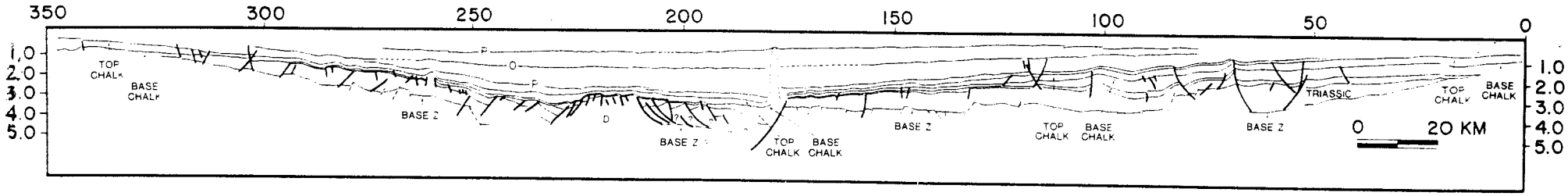


Figure 14: A drawing of the NOPEC seismic line emphasizing the mid-Jurassic through early Cretaceous and Permo-Triassic faulting.

TABLE 4

COMPARISON OF EXTENSION FROM FAULTING AND SUBSIDENCE, MID-JURASSIC THROUGH EARLY CRETACEOUS AND PRE-JURASSIC EXTENSION.

| DISTANCE (KM)[1] | 350-250 | 250-150 | 150-50 |
|---|---|---|---|
| EXTENSION FROM MID-JURASSIC THROUGH EARLY CRETACEOUS FAULTS[2] | 4 | 22 | 7 |
| EXTENSION FACTOR $\beta$ FROM FAULTS | 1.04 | 1.28 | 1.08 |
| EXTENSION FACTOR $\beta$[3] FROM SUBSIDENCE | 1.09-1.14 | 1.24-1.43 | 1.07-1.17 |
| EXTENSION FROM TRIASSIC FAULTING[2] ASSUMING EAST WEST EXTENSION | 3 | -- | 5 |
| EXTENSION FACTOR $\beta$[3] FROM SUBSIDENCE ASSUMING HALF THE PRE JURASSIC EXTENSION OCCUR IN THE TRIASSIC[4] | 1.06-1.10 | 1.27-1.35 | 1.16-1.21 |

[1] DISTANCE ALONG CROSS SECTION (FIGURE 10)

[2] EXTENTION EQUALS SUM OF HORIZONTAL DISPLACEMENT OF FAULT BLOCKS ALONG VISIBLE HIGH-ANGLE FAULTS WITHIN GIVEN RANGE OF CROSS SECTION.

[3] AVERAGE OF EXTENSION FACTORS (TABLE 2) FOR SITES WITHIN GIVEN DISTANCE RANGE. MEASURED BY PROJECTING WELLS SHOWN AS FIGURE 3A ONTO THE SEISMIC LINE, FIGURE 10. (350-250 KM: SITES 1, 2, 3; 250-150 KM: SITES 4, 5, 6; 150-50 KM: SITES 7, 8, 9, 10).

[4] THIS EXTENSION DOES NOT HAVE TO BE EAST WEST, IT COULD BE NORTH SOUTH AND REPRESENTS LESS THAN 20 KMS OF OFFSET ALONG MAJOR FAULTS.

Our analysis of the throw on the high angle faults is preliminary as we have used only a time section. We do not have the data to justify creating a depth section, make allowances for compaction and reconstructing the original configuration of the faults assuming a balanced section (Gibbs, 1984). These techniques have been applied to the Witchground graben by Beach (1984). They increased the predicted extension over the extension determined by analyzing the time section alone.

The reflection seismic line presents evidence for substantial thinning and even absence of Jurassic, Triassic and possibly earlier sediments in and on the flanks of the Central Graben. It is generally accepted that the absence of sediments is due to erosion during mid-Jurassic uplift. Estimates of the magnitude of this uplift vary greatly, from 60 to 2000 m (Ziegler, 1982). From arguments based on sediment mass balance in the area we prefer the 250 m figure of uplift (Leeder, 1983) for the removal of Permian and Triassic sediments. The mid-Jurassic uplift on the flanks fo the graben can be accounted for by non-uniform extension (Salveson, 1978; Leeder, 1983; Hellinger and Sclater, 1983) where more distributed extension in the lower lithosphere causes extensive uplift on either side of the region of crustal extension.

There is agreement between the fault derived and crustal thickness and sediment fill derived extension factors for the mid-Jurassic through early Cretaceous phase of extension. However, no such agreement appears to exist for the earlier phases. The corresponding crustal thinning and subsidence derived extension factors indicate at most 100 km of extension across the 350 km of profile if the extension is east-west. There is little evidence for more than 10 km of east-west extention in either the Permian or the Triassic on the actual profile (Figure 14; Table 4). The base Zechstein salt is a major reflector clearly visible on the seismic line. It is

nearly continuous on either side of the graben and there is evidence for significant high angle faulting only in the Egersund basin in eastern portion of the section. The graben itself has been too disturbed by the later phase of extension for calculations of Permian and Triassic extension to be made within the graben. However, even if extension were very great in the graben, the effect would still not be large enough to account for either the Permian or Triassic subsidence.

The absence of visible high-angle east-west trending faults in either the Permian or the Triassic presents a problem to the application of extensional models to the subsidence of the North Sea basin. It is especially true for this basin as the mid-Jurassic through early Cretaceous faulting is so obvious. However, the parameters derived assuming crustal thinning by extension give an excellent match to the subsidence history of the basin. The extensional framework cannot be rejected outright and explanation needs to be sought for the absence of visible high-angle faulting in the earlier phases.

The mid-Jurassic through early Cretaceous rifting was dominantly east-west in direction and has produced roughly north-south trending basins. In contrast both the Permian and Triassic basins are lineated east-west (Figures 5a and 5b) and lie approximately at right angles to the trend of the later phase of rifting (Figure 3a). The northern of the two Permian basins is less extensive and much less deep than the basin to the south. Evidence for limited Permian extension in the North Sea region has been reported by Glennie (1983) and Bradley, et al., (1984). Currently the evidence for the late Carboniferous and early Permian extension is mixed. Clearly there has been a major igneous event in the Stephanian-Autunian under the South Permian basin. However it is not clear how extensive this

event was beneath the North Permian basin. Salveson (in press) and to a degree Ziegler (1982) argue for a major event that totally reset the thermal structure of the lithosphere. There are difficulties with such a model as the subsidence rates in the Permian basins are close to oceanic and it is difficult to create the required reheating without substantial extension and massive intrusion which would in itself create much of the subsidence. We argue that this thermal destabilization is associated principally with wrench faulting in the Stephanian. Further, we suggest that these faults are not visible on the multichannel seismic lines due to their sense of direction, depth and the salt cover.

Extension in the Triassic is relatively easy to justify (Ziegler, 1982) as there are many active faults observed during this time interval (Pegrum, 1984) (Figure 15a). However, few of the faults appear to be associated with north south extension. They all appear to be lineated east west and have been interpreted as wrench faults. The Triassic basin is relatively narrow. Thus, a relatively small event, possibly associated with transtension along the continuation of the Tornquist zone proposed by Pegrum (1984) (Figure 15b) could produce roughly fifteen to twenty kilometers of extension. Such a stretching event could account for all the Triassic sedimentary fill. Evidence for this extension could have been removed by more recent faulting and or salt movement.

We suggest that such extension in the Triassic and the wrench faulting and intrusion in the Stephanian and Autunian can account for the values computed for the pre Jurassic extension. Because this faulting does not have to be extensive we argue that it could be hidden by the sense of direction and the depth. In addition the significant salt cover and salt movement beginning in the Triassic would make this extension difficult to detect.

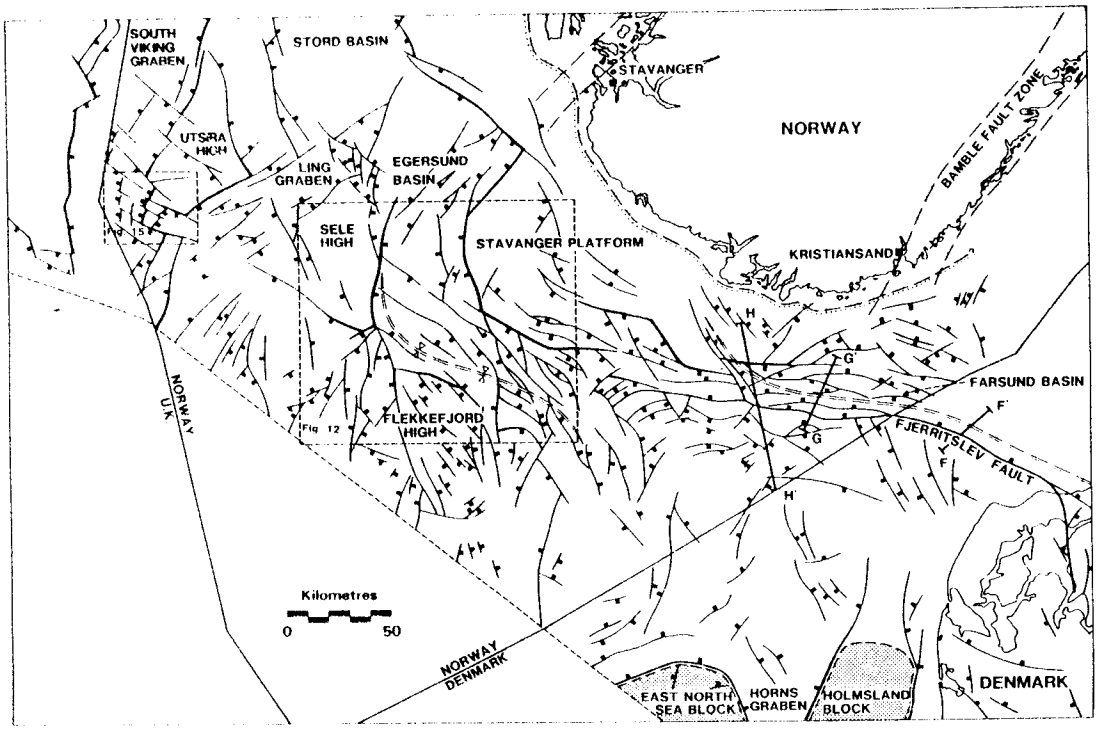


Figure 15a. The structural framework of the southern Norwegian North Sea, Light stipple: Pre-Mesozoic rocks at surface; dark stipple: positive structural blocks in the subsurface. (From Pegrum, 1984a.)

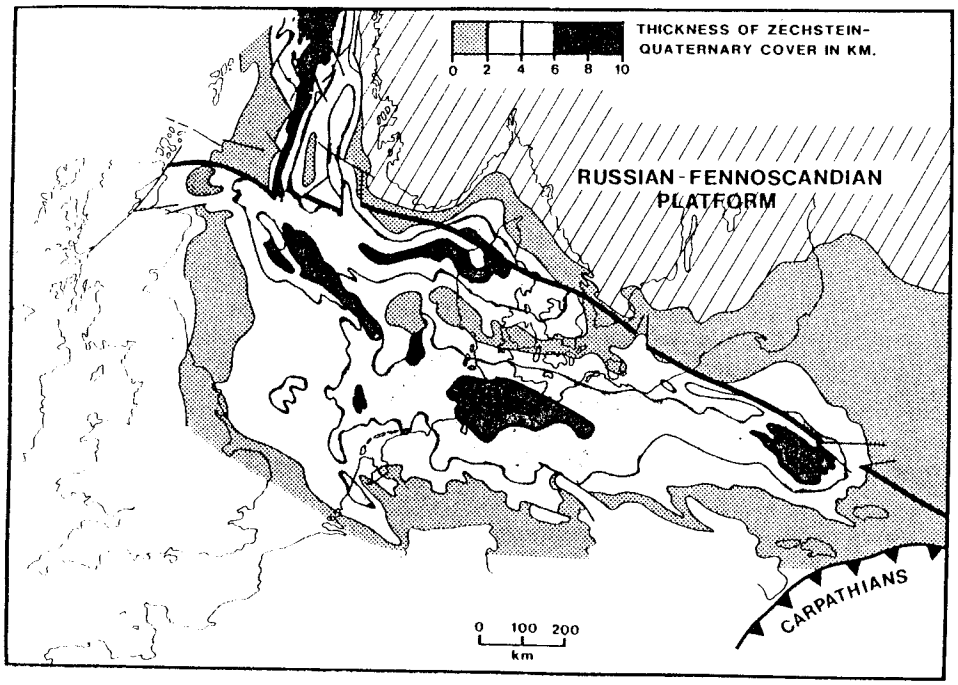


Figure 15b. Relationship between the Tornquist Zone and the distribution of Upper Permian to Quaternary sediments in northern Europe. (From Pegrum, 1984b.)

There is a problem with the absence of evidence for Triassic extension. However, there is a lack of definition of the exact extent of the pre Jurassic extensional events. Thus we do not believe that this problem is sufficiently major to reject a model based on the observed tectonic history that accounts for both the observed crustal thinning and sediment fill and gives the observed burial history for the basement. Further, this model involves extension along normal faults which could or could not be high angle. Thus we do not believe there is any necessity to invoke the reactivation of low angle normal faults or an igneous event of unknown magnitude to account for the subsidence of the Central North Sea basin.

## CONCLUSIONS

Since the end of the Carboniferous there have been three major epochs of sedimentation in the Central North Sea basin; the first covered the Permian, the second, the Triassic and the third, the mid-Jurassic to present. Wood and Barton (1983) and Barton and Wood (1984) have shown that the crust is thinner under the central basin than under the continents on either flank. Also the principal area of crustal thinning is the region of thickest sediment cover.

If it is assumed that the thinned crust is caused by extension then the amount of extension can account for the observed sediment fill and the overall distribution of the sediment layers. We follow the overall geologic history of the area given by Ziegler (1982) and separate this extension and thermal destabilization into Stephanian-Autunian, Triassic and mid-Jurassic through early Cretaceous phases. A simple time dependant extensional model (Jarvis and McKenzie, 1980) based on this history can account for the subsidence history at five sites in the Central basin.

We have analyzed a multichannel seismic line run close to the refraction profile and wells presented by Barton and Wood (1983). The amount of extension predicted by the crustal thinning, sedimentary fill and subsidence arguments is observed for the mid-Jurassic and early Cretaceous phase. It is on the order of 30-40 kms. However, no evidence is found for high-angle faulting on the regionally correlatable base Zechstein reflector which is clearly visible on eighty percent of the reflection profile. As had been pointed out by Ziegler (1983) the absence of clear evidence of pre-Jurassic extension is a problem to any model using extension as the basic method of accounting for the subsidence of the North Sea basin.

The three phase extensional model gives excellent predictions of the crustal thinning, total sediment fill and subsidence history. It should not be rejected at this time because of the apparent absence of pre Jurassic faulting on the seismic line. There is alternative evidence of at least two stages of faulting between the late Carboniferous and Jurassic. Extension during these stages does not have to be too large to explain the subsidence. Such a limited amount of extension would be difficult to detect on east west seismic lines because of its sense of direction. The depth of the faulting in the section, the salt cover and or salt motion at a later date would all add to the detection problems.

Future applications of extensional models to the North Sea basin should concentrate on the total Carboniferous section in areas of minimal pre-Permian subsidence, not just on the mid-Jurassic section. The studies should concentrate on (a) the possibility of extension in the late Carboniferous and the Triassic and (b) seismic profiles, both refraction and deep crust reflection at right angles to the major axes of the pre Jurassic basins.

ACKNOWLEDGMENTS

We are grateful to Peter Ziegler of Shell International Petroleum Company for repeatedly bringing to our attention the discrepancies between the observations and the predictions from the extensional models. H. Carstens gave us permission to publish a recent NOPEC 'spec-shoot' seismic reflection line acquired by GECO across the Central Graben of the North Sea. A. Bally and scientists from Phillips Petroleum Company aided us with the interpretation of this line. We thank B. Celerier for his comments on an earlier version of this manuscript.

This work was supported by a Shell Company Foundation Professorship awarded to the senior author.

## REFERENCES


Badley, M. E., Egeberg, T., Nipen, O., 1984. Development of rift basins illustrated by the structural evolution of the Oseberg feature, Block 30/6, offshore Norway, J. Geol. Soc. London, 141, 639-649.

Bally, A. W., 1984. Structural styles and the evolution of sedimentary basins, Amer. Assoc. Petrol. Geol., short course notes, Rice University, Houston, pp. 238.

Beach, A., 1984. Structural evolution of the Witch Ground Graben, J. Geol. Soc. London, 141, 621-628.

Barton, P. J., and Matthews, D. H., 1984. Deep structure and geology of the North Sea region interpreted from a seismic refraction profile. Annales Geophysicae, 2(6), 663-668.

Barton, P. and Wood, R., 1984. Tectonic evolution of the North Sea basin: crustal stretching and subsidence, Geophys. J. R. astr. Soc., 79, 987-1022.

Barton, P., Matthews, D. H., Hall, J., and Warner, M., 1984. Moho beneath the North Sea compared on normal incidence and wide-angle seismic records. Nature, 308, 5954, 55-56.

Calcagnile, G., 1982. The lithosphere-asthenosphere system in Fennoscandia, Tectonophysics, 90, 19-35.

Day, G. A., Cooper, B. A., Andersen, C., Burgers, F. J., Ronnevik, H. C. and Schoneich, H., 1981. Regional seismic structure maps of the North Sea in Petroleum Geology of the Continental Shelf of North-West Europe, Institute of Petroleum: London, Illing, L. V. and Hobson, G. D., eds., 76-84.

Donato, J. A., and Tully, M. C., 1981. A regional interpretation of North Sea gravity data, in Petroleum Geology of the Continental Shelf of North-West Europe, Institute of Petroleum: London, Illing, L. V. and Hobson, G. D., eds., 76-84.

Fowler, C., 1974. The geology of the Montrose field, 1975, in Petroleum and the Continental Shelf of North-West Europe, ed. by A. W. Woodland, John Wiley and Sons, 467-476.

Glennie, K. W., 1984. The Structural Framework and the Pre-Permian History of the North Sea Area, in Introduction to the Petroleum Geology of the North Sea, ed. K. W. Glennie, 17-49, Blackwell Scientific Publications, London.

Hellinger, S. J., and Sclater, J. G., 1983. Some comments on two-layer extensional models for the evolution of sedimentary basins, J. Geophys. Res., 88, B10, 8251-8269.

Hellinger, S. J., Sclater, J. G. and Shorey, M., (in press). Pre-Jurassic extension: a major feature in the subsidence of the North Sea Basin, submitted to Nature, Dec. 1985.

Hellinger, S. J., Shedlock, Sclater, J. G., and Hong, Y., 1985. The Cenozoic Evolution of the North China Basin, Tectonics, 4, 2, 171-185. Tectonics.

Jarvis, G. T., and McKenzie, D. P., 1980. Sedimentary basin formation with finite extension rates, Earth Planet. Sci. Lett., 48, 42-52.

Parsons, B. and Sclater, J. G., 1977. An analysis of ocean floor bathymetry and heat flow with age, J. Geophys. Res., 82, 803-827.

Leeder, M. R., 1983. Lithospheric stretching and North Sea Jurassic clastic sonreelants, Nature, 305, 510-514.

McKenzie, D., 1978. Some remarks on the development of sedimentary basins, Earth and Planet, Sci. Lett., 40, 25-32.

Royden, L., and Keen, C., 1980. Rifting process and thermal evolution of the continental margin of Eastern Canada determined from subsidence, Earth Planet. Sci. Lett., 51, 343-361.

Royden, L., Sclater, J. G., and Von Herzen, R. P., 1980. Continental margin subsidence and heat flow: important parameters in formation of petroleum hydrocarbons, Amer. Assoc. Petrol. Geol. Bull., 64(2), 173-187.

Pegrum, R. M., (1984a). The extension of the Tornquist Zone in the Norwegian North Sea., Norsk Geologisk Tidsskrift, 64, 39-68.

Pegrum, R. M., (1984b). Structural development of the southwestern Margin of the Russian-Fennoscandian Platform, in Petroleum Geology of the North European Margin, eds., Graham and Trotman, Norwegian Petroleum Society, pp. 359-369.

Royden, L., Horvath, F., and Rumpler, J., 1983. Evolution of the Pannonian Basin System, Tectonics, 2(1), 63-90.

Salveson, J. O., 1978. Variations in the geology of rift basin - A tectonic model, paper presented at Rio Grande Rift Symposium, Santa Fe, N. M., Oct., 1978.

Sclater, J. G. and Christie, P. A. F., 1980. Continental stretching - an explanation of the post mid-Cretaceous subsidence of the central graben of the North Sea. J. Geophys. Res., 85, 3740-3750.

Selley, R. C., 1978. Porosity gradients in North Sea oil-bearing sandstones, Geol. Soc. London, 135, 119-132.

Sorenson, K., (in press). Triassic subsidence of the Danish Basin, Nature.

Van Eysinga, F. W. B., 1975. Geological time table. Elsevier Publishers, Amsterdam.

Wood, R. J., 1981. The subsidence history of Conoco well 15/30-1, central North Sea. Earth and Planet. Sci. Lett., 54, 306-312.

Wood, R. and Barton, P., 1983. Crustal thinning and subsidence in the North Sea, Nature, 302 (5904), 134-136.

Ziegler, P. A., 1977. Geology and hydrocarbon provinces of the North Sea. GeoJournal, 1, 7-32.

Ziegler, P. A., 1978. North-western Europe: Tectonics and basin development. Geologie en Mijnbouw, 57, 589-626. Ziegler, P. A., 1981. Evolution of sedimentary basins in North-West Europe in Petroleum Geology of the Continental Shelf of North-West Europe, The Institute of Petroleum: London, Illing, L. V. and Hobson, G. D., eds., 3-42.

Ziegler, P. A., 1982. Geological Atlas of Western and Central Europe, Shell International Petroleum, Maatschappij B. V.

Ziegler, P. A., 1983. Crustal thinning and subsidence in the North Sea, Nature, 304, 561.